Article

Baleen whale prey consumption based on high-resolution foraging measurements

https://doi.org/10.1038/s41586-021-03991-5

Received: 5 July 2020

Accepted: 1 September 2021

Published online: 3 November 2021

Check for updates

Matthew S. Savoca[1]✉, Max F. Czapanskiy[1], Shirel R. Kahane-Rapport[1], William T. Gough[1], James A. Fahlbusch[1,2], K. C. Bierlich[3,4], Paolo S. Segre[1], Jacopo Di Clemente[5,6,7], Gwenith S. Penry[8], David N. Wiley[9], John Calambokidis[2], Douglas P. Nowacek[3], David W. Johnston[3], Nicholas D. Pyenson[10,11], Ari S. Friedlaender[12], Elliott L. Hazen[1,12,13] & Jeremy A. Goldbogen[1]

Baleen whales influence their ecosystems through immense prey consumption and nutrient recycling[1–3]. It is difficult to accurately gauge the magnitude of their current or historic ecosystem role without measuring feeding rates and prey consumed. To date, prey consumption of the largest species has been estimated using metabolic models[3–9] based on extrapolations that lack empirical validation. Here, we used tags deployed on seven baleen whale (Mysticeti) species (n = 321 tag deployments) in conjunction with acoustic measurements of prey density to calculate prey consumption at daily to annual scales from the Atlantic, Pacific, and Southern Oceans. Our results suggest that previous studies[3–9] have underestimated baleen whale prey consumption by threefold or more in some ecosystems. In the Southern Ocean alone, we calculate that pre-whaling populations of mysticetes annually consumed 430 million tonnes of Antarctic krill (*Euphausia superba*), twice the current estimated total biomass of *E. superba*[10], and more than twice the global catch of marine fisheries today[11]. Larger whale populations may have supported higher productivity in large marine regions through enhanced nutrient recycling: our findings suggest mysticetes recycled 1.2×10^4 tonnes iron yr^{-1} in the Southern Ocean before whaling compared to 1.2×10^3 tonnes iron yr^{-1} recycled by whales today. The recovery of baleen whales and their nutrient recycling services[2,3,7] could augment productivity and restore ecosystem function lost during 20th century whaling[12,13].

Top predators have direct effects on their prey that translate to indirect effects on ecosystem structure, function and productivity[1,2,14,15]. Understanding the causes and consequences of these effects depends on direct measurements from large vertebrates, which are logistically challenging to collect, particularly for species threatened with extinction[16,17]. Extant baleen whales (or mysticetes) are the largest animals of all time and typically forage on dense patches of small fish or crustaceans by either continuous ram filtration (for example, balaenid whales) or intermittent lunge filtration (for example, rorqual whales)[18]. For most terrestrial or amphibious vertebrates, prey consumption has been calculated from direct observations; however, in modern oceans, baleen whales frequently forage well below the surface (Fig. 1) and cannot be held in captivity, precluding direct measurements of ingestion rates. Scientists have spent a century estimating the prey requirements of baleen whales using a variety of approaches (see Methods), but direct measurements to improve or validate these estimates have been unavailable. However, recent advances in bio-logging and fisheries acoustics have enabled direct measures of feeding rates and prey density of the largest whales in their natural environment.

Previously, mysticete prey consumption has been estimated from bioenergetic models, extracting and weighing stomach contents from harvested whale carcasses, or a combination of the two approaches (see Methods). For the former, studies assumed a 1:3 ratio of basal metabolic rate to field metabolic rate (based on Kleiber's 'three-quarter' law[19]) to determine caloric requirements to meet metabolic demands[4,5], but the estimated metabolic rates of the largest animals remain unvalidated by field data. Typically, empirical field metabolic rates are limited to animals several orders of magnitude smaller than mysticetes, with disparate physiology and evolutionary histories[20]. Stomach contents collected from whaling have been used to estimate total prey consumption on daily and annual scales, but these data lack associated digestion times (that is, gastrointestinal motility), feeding rates (that is, lunges h^{-1}), and measures of prey patch density (that is, the average biomass in krill swarm or fish school). Despite these knowledge gaps, current consensus suggests that mysticetes consume ≤5% of their body weight per day when feeding (Extended Data Figure 1; see Methods).

Mysticetes ingest large quantities of prey and egest their remains in the photic zone, thereby facilitating nutrient recycling and retention in

[1]Hopkins Marine Station, Stanford University, Pacific Grove, CA, USA. [2]Cascadia Research Collective, Olympia, WA, USA. [3]Duke University Marine Laboratory, Duke University, Beaufort, NC, USA. [4]Marine Mammal Institute, Hatfield Marine Science Center, Oregon State University, Newport, OR, USA. [5]Department of Biology, University of Copenhagen, Copenhagen, Denmark. [6]Department of Biology, University of Southern Denmark, Odense, Denmark. [7]Department of Bioscience, Aarhus University, Aarhus, Denmark. [8]Institute for Coastal and Marine Research, Nelson Mandela University, Port Elizabeth, South Africa. [9]Stellwagen Bank National Marine Sanctuary, NOAA National Ocean Service, Scituate, MA, USA. [10]Department of Paleobiology, National Museum of Natural History, Washington, DC, USA. [11]Department of Paleontology and Geology, Burke Museum of Natural History and Culture, Seattle, WA, USA. [12]Long Marine Laboratory, University of California, Santa Cruz, Santa Cruz, CA, USA. [13]Environmental Research Division, NOAA Southwest Fisheries Science Center, Monterey, CA, USA. ✉e-mail: msavoca@stanford.edu

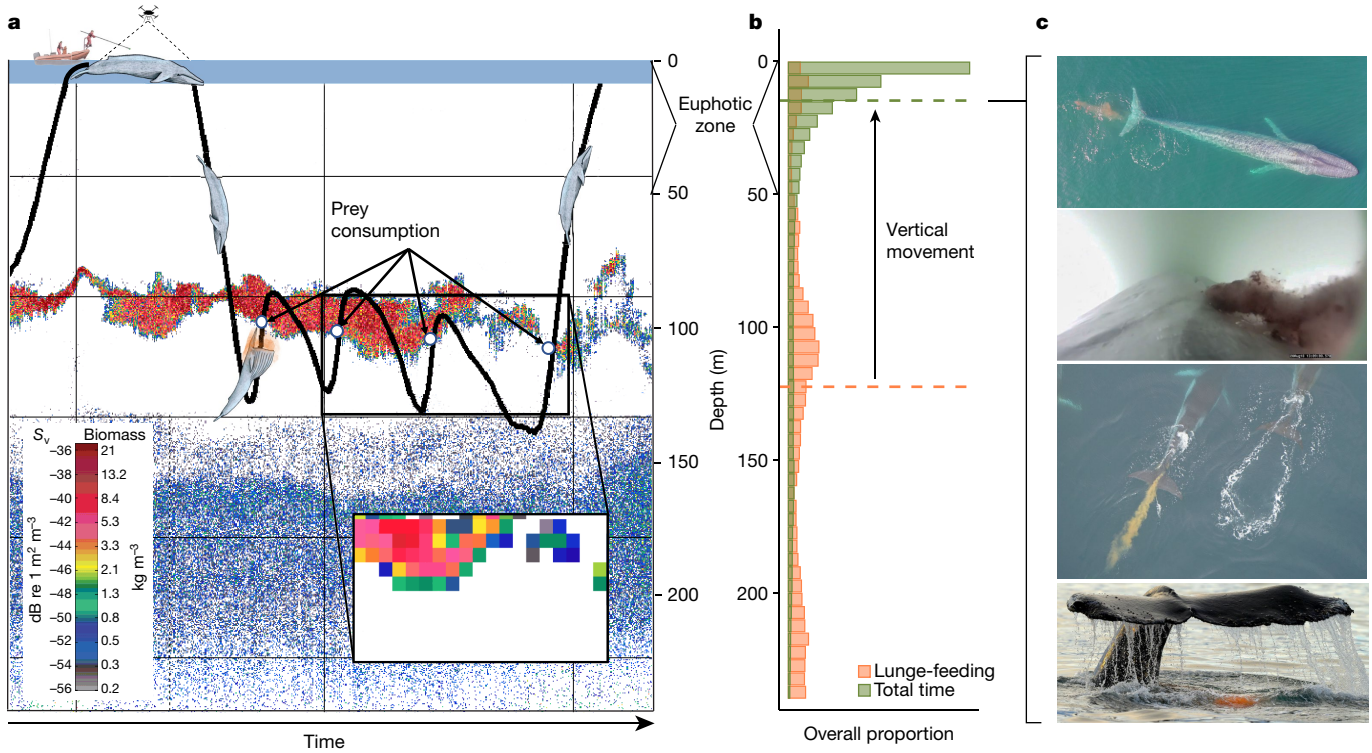

Fig. 1 | Field measurements informing baleen whale prey consumption and nutrient recycling. a, Schematic illustrating fieldwork—tagging, drone measurements and prey mapping—highlighting an example of one dive of an eastern North Pacific (ENP) blue whale (*B. musculus*). Its dive profile (black line) and prey consumption (that is, lunge-feeding) events are indicated with unfilled blue circles. The colour scale bar in the bottom left represents acoustic or echogram values in mean volume backscattering strength (S_v in units of dB re 1 m^2 m^{-3}) and its translation to krill biomass (in units of kg m^{-3}). Inset on the bottom right shows bin-averages of raw echosounder output into gulp-sized cells in krill biomass units for prey-consumption analysis (see Methods for details). Typical depth of the euphotic zone in this ecosystem is ~50 m (ref. [49]). **b**, Vertical histogram showing lunge-feeding events (orange) for tagged ENP blue whales by depth with median feeding depth (dashed orange line). Total time-by-depth plot over a full day (green bars), and median depth of ENP blue whales (dashed green line). The difference between the orange and green dashed lines is the estimated vertical movement of nutrients by an ENP blue whale. **c**, Images of baleen whales recycling nutrients. From top to bottom: an ENP blue whale in 2019, a still image from a tag video of an ENP fin whale (*B. physalus*) defecating underwater in 2018, an Antarctic minke whale (*B. bonaerensis*) in the West Antarctic Peninsula in 2018, a humpback whale (*M. novaeangliae*) in the West Antarctic Peninsula in 2014. Photos by the authors under NOAA permits 16111, 14809, 23095, and ACA permits 2015-011 and 2020-016.

the epipelagic[21] (Fig. 1). This recycling of limiting nutrients from mysticetes to primary producers has the capacity to boost the intensity and extent of phytoplankton blooms, in both space and time, thus influencing ecosystem dynamics[3,15]. In the Southern Ocean, mysticete abundance declined dramatically from 1910–1970 due to industrial whaling, and the functional extinction of large whales preceded reductions of primary productivity and krill biomass in the region[22,23]. To anticipate ecosystem responses from past to present, we generated a global dataset of consumption rates from field data on half of all extant mysticete species (Extended Data Table 1, Extended Data Figure 2). We calculated estimates of daily foraging behaviour (based on feeding events and filtration rates of prey-laden water in m^3 d^{-1}) and prey consumption (kg prey ingested d^{-1}). We used these data to estimate the amount of prey consumed (in Mt yr^{-1}) and iron recycled (in tonnes yr^{-1}) by Southern Ocean mysticete populations. These calculations provide the basis for estimating ocean ecosystem function before and after whaling, highlighting the benefits of mysticete population recovery in the 21st century.

Results and discussion

Mysticete prey consumption and water filtration

We used data from 321 tag deployments on seven mysticete species in three oceans, including 292 deployments on rorquals (comprising 74,247 lunge-feeding events), and 29 deployments on two balaenid species (Extended Data Fig. 2, Extended Data Table 1; see Methods). For the rorqual whales, drone photogrammetry and allometric equations allowed us to estimate engulfment capacity[24] (Extended Data Fig. 3; Extended Data Table 1). Concurrently, we measured krill density (that is, biomass per m^3) for patches on which these whales were foraging[25] (Fig 1; Extended Data Table 1, Extended Data Fig. 3; see Methods). We found that, on feeding days, an adult eastern North Pacific (ENP) blue whale (*Balaenoptera musculus*; measured median length: 22.4 m) is likely to consume 16 tonnes d^{-1} (10–22 tonnes d^{-1}; median and Q1–Q3 range, the 25th–75th percentile) of krill, primarily *Thysanoessa spinifera*[26] (Fig. 2, Extended Data Table 1). By comparison, a continuous ram-feeding North Atlantic right whale (*Eubalaena glacialis*; adult length 13–16 m) ingests 5 tonnes d^{-1} (Q1–Q3 range, 2–8 tonnes d^{-1}) of small zooplankton (for example, copepods), and a bowhead whale (*Balaena mysticetus*; adult length 15–19 m) ingests 6 tonnes d^{-1} (Q1–Q3 range, 3–13 tonnes d^{-1}) of small zooplankton (Extended Data Fig. 4, Extended Data Table 1). Across all species and regions, median daily prey consumption was calculated to be 5–30% of body mass per day when feeding, dependent on prey type. These results are threefold higher than previous estimates on average[4,6,27] (see Methods, Fig. 3, Extended Data Fig. 1). On a mass-specific basis, mysticetes also consume more than previously assumed across all species, regions and prey types. Mass-specific energy intake decreases with body size from humpback whales to blue whales feeding on krill in the ENP (Extended Data Fig. 5e, f). In addition, consistent energetic intake was seen in populations that

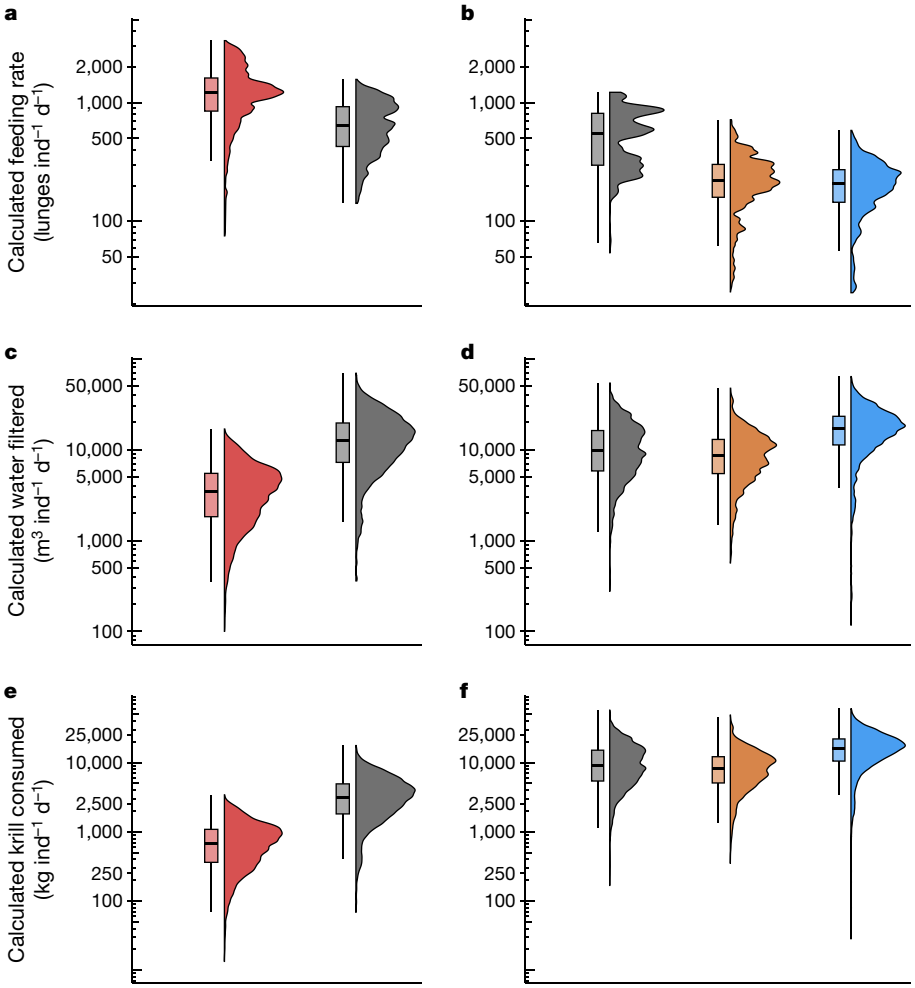

Fig. 2 | Individual rorqual daily feeding rate, water filtered and krill consumed. Each column displays modelled daily feeding rates, filtration volumes and prey consumption on a log scale for the species depicted. **a**, **c**, **e**, The left column displays estimates from Antarctic minke (*B. bonaerensis*) and humpback whales (*M. novaeangliae*) from the West Antarctic Peninsula. **b**, **d**, **f**, The right column displays estimates from humpback, fin (*B. physalus*), and blue whales (*B. musculus*) from the eastern North Pacific. Density plots illustrate the full scope of all daily simulations with the height representing the relative probability of each output; the boxplots show the quartiles of these outputs with the thick line representing the median and the shaded region representing the Q1–Q3 range (25th–75th percentiles) of all modelled daily rates.

prey-switch—such as ENP humpback whales (*Megaptera novaeangliae*) feeding on anchovy (*Engraulis mordax*) or krill (*T. spinifera* and *Euphausia pacifica*)—despite considerable differences in feeding rates and prey biomass ingested (Extended Data Fig. 5e, f). The ability to forage on multiple prey types with similar net energy gain may buffer generalist predators against increased ocean variability under climate change[28].

Our estimates of mysticete water filtration suggest that the ecological influence (for example, via biomixing[29]) of these top predators has also been underestimated. A single intermittent lunge-feeding blue whale filters 17,000 m^3 d^{-1} (Q1–Q3 range, 11,000–23,000 m^3 d^{-1}; Fig. 2), while a continuous ram feeding balaenid whale filters four times that amount (Extended Data Fig. 4). Among rorquals, krill-feeders filtered considerably more water than fish-feeders due to higher lunge rates on less mobile prey (Fig. 2). Compared to filter feeding fish and invertebrates[30–32], mysticetes process a similar amount of water per hour on a mass-specific basis.

These data allowed us to project annual water filtration and prey consumption by rorqual individuals and populations at regional to global scales (Figs. 3, 4). Our analyses found that in regions such as the ENP, krill consumption has been underestimated. For example, Barlow and colleagues[4] estimated that all cetaceans in the California Current Ecosystem (22 spp.) require ~2 Mt yr^{-1} of prey including fish, krill and cephalopods. In contrast, we find that blue, fin (*Balaenoptera physalus*) and humpback whale populations in this ecosystem each require >2 Mt yr^{-1} of krill. Annually, an individual humpback-sized (10–15 m) rorqual filters approximately one million cubic meters of water. At the population level, the filtration capacity of Northern Hemisphere rorquals have been cut in half by whaling, from 200 to 100 km^3 yr^{-1}; whereas in the Southern Ocean, whaling has reduced this effect approximately tenfold, from 2,000 to 200 km^3 yr^{-1} (Fig. 4). Globally, filtration by the largest mysticetes—blue, fin, right and bowhead whales—has decreased by >90% in the past century. In particular, the annual filtration by Southern Ocean blue whales declined 99% since the start of industrial whaling (Fig. 4). In the Northern Hemisphere, the greatest reductions in filtration and prey consumption resulted from fin whale removal, whereas in the Southern Hemisphere the greatest losses resulted from the near extirpation of blue whales (Fig. 4).

Industrial whaling and ecosystem productivity

Our higher-than-expected prey consumption and filtration estimates suggest that the role of mysticetes in ocean ecosystems has been underestimated. To assess the impact of whaling on ecosystem productivity

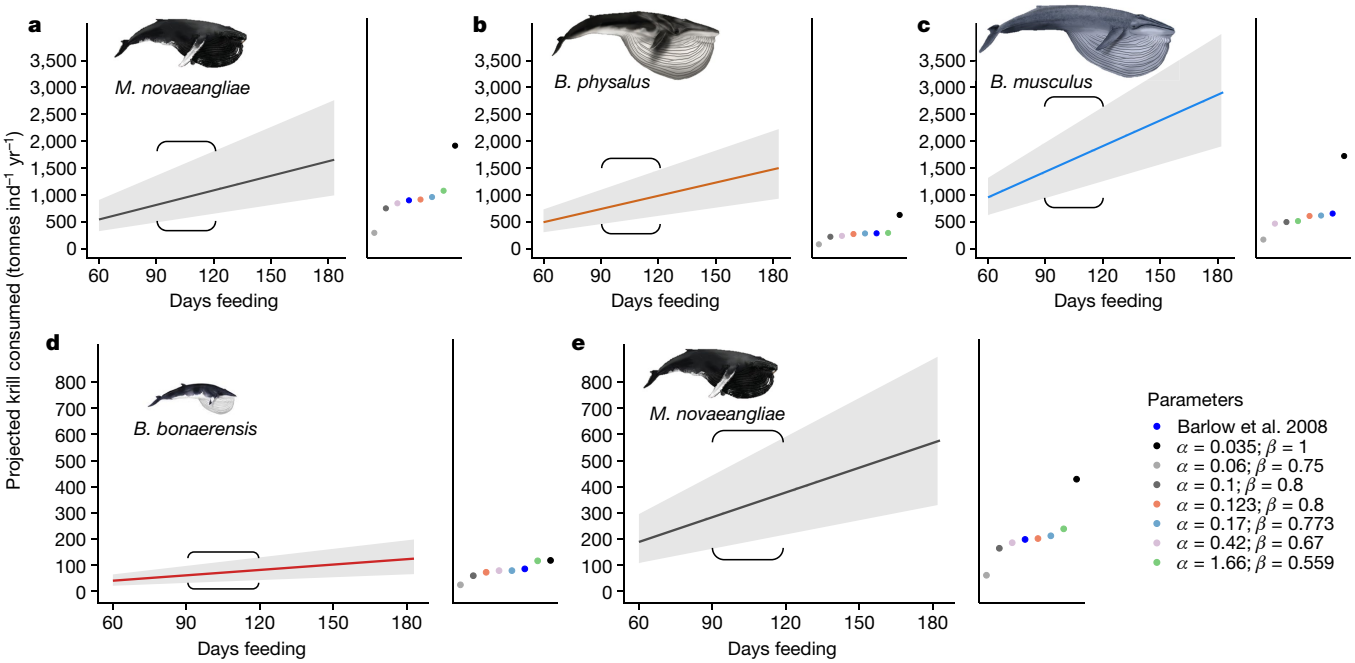

Fig. 3 | Individual annual prey consumption estimates, with comparison to prior estimates. Dots represent prey consumption estimates from prior studies (see Extended Data Table 3 for references). The solid lines represent annual prey consumption estimates for an individual whale for a given number of days feeding (range, 60–182.5 days) using a conservative metric of prey consumption (see Methods); solid line is the median; grey bars represent the Q1–Q3 range. Bracketed regions represent the most likely annual consumption per individual, represented by 90–120 feeding days. **a**–**c**, The coloured lines represent the projected annual krill consumption by an individual humpback (*M. novaeangliae*), fin (*B. physalus*) or blue whale (*B. musculus*) from the eastern North Pacific. **c**–**e**, The solid curved lines represent the median projected annual krill consumption by an individual Antarctic minke (*B. bonaerensis*) or humpback whale in the West Antarctic Peninsula.

we focused on Southern Ocean rorquals because they primarily subsist on one well-studied prey species (Antarctic krill, *E. superba*) and the majority of mysticetes killed by humans were Southern Ocean rorquals from the early to mid-20th century[33,34]. In total, 1.5 million of the 2 million rorquals killed in the 20th century were removed from the Southern Ocean, with the largest species facing the greatest exploitation[33,34]. Blue whales suffered the greatest relative defaunation and, as a result, estimates of population-level krill consumption declined 99.6%, from 167 Mt yr^{-1} in 1900 to 0.6 Mt yr^{-1} in 2000 (Fig. 4). The annual krill surplus resulting from whale removal (that is, the biomass of krill, *E. superba*, left unconsumed annually by all whale species) is estimated at 379 Mt yr^{-1} (Q1–Q3 range, 175–422 Mt yr^{-1}), more than twice what was first predicted by Laws[35] (150 Mt yr^{-1}; Fig. 4). Unconsumed krill left behind by each of the two largest species—fin (143 Mt yr^{-1}; Q1–Q3 range, 66–161 Mt yr^{-1}) and blue whales (166 Mt yr^{-1}; Q1–Q3 range, 79–178 Mt yr^{-1})—is as much or greater than the originally predicted krill surplus[35].

Whaling was expected to have resulted in net increases in both whale prey and competing predator species, due to predatory and competitive release, respectively (that is, the 'krill-surplus hypothesis')[35]. Instead, the opposite has happened (that is, the 'krill paradox'). Since the mid-20th century, populations of seabirds, predatory fish and other marine mammals have largely remained stable or declined at regional and global scales[34,36–38]. Unexpectedly, krill biomass has declined sharply (>80%) on the former whaling grounds—the southwest Atlantic sector of the Southern Ocean—post-whaling[22]. At the beginning of the 20th century, Southern Hemisphere populations of Antarctic minke (*Balaenoptera bonaerensis*), humpback, fin and blue whales consumed twice as much Antarctic krill as was estimated to exist at the end of the 20th century (215 Mt yr^{-1}; see Methods)[10], suggesting that historic krill biomass must have been far greater than at present. More broadly, pelagic production at high latitudes ranks among the highest in the world ocean[39], and this production was likely to be even more substantial before industrial whaling. Pre-whaling populations of Southern Ocean mysticetes may have enhanced the location, duration and intensity of primary production by catalysing nutrient availability to the base of marine food webs.

Our findings suggest that ecosystem models underestimate the quantity of prey consumed and ecosystem services provided by current and historic populations of baleen whales[21,40]. For example, Ratnarajah et al.[40] found that iron fertilization by baleen whales probably occurred only when mysticete prey consumption and defecation rates in the photic zone were maximized. Our results imply that even their highest assumptions for these parameters underestimates reality. Additionally, the presence of numerous foraging mysticetes in historic oceans has been hypothesized to reduce diel migrations of krill[41], which could further increase krill and whale defecation and mixing in the photic zone. Competition for prey between whales and commercially harvested fish has led to the hypothesis that large whale populations and modern fisheries could not coexist[42,43]. However, competition between whales and fisheries may be offset by whale-recycled nutrients to the base of the food web[3,7,21].

In the Southern Ocean, pre-whaling populations of Antarctic minke, humpback, fin and blue whales could recycle between 0.7 and 1.5×10^4 tonnes Fe yr^{-1} (Q1–Q3 range) to iron-limited phytoplankton (Fig. 4c). One quarter of iron released by whales may have been incorporated by phytoplankton[40]. This, in turn, could increase net primary productivity (NPP) by 215 TgC yr^{-1} (range, 27–1,459) across the Southern Ocean, ~11% of Southern Ocean NPP estimates from the end of the 20th century[44] (see Methods; Extended Data Table 2). In sections of the Southern Ocean where mysticetes were more numerous (for example, the Scotia Sea), whale-recycled iron may have catalysed >20% more NPP than at present. Elsewhere, nutrient recycling provided by whales could operate in regions limited by macronutrients, such as nitrogen or phosphorous[2,3].

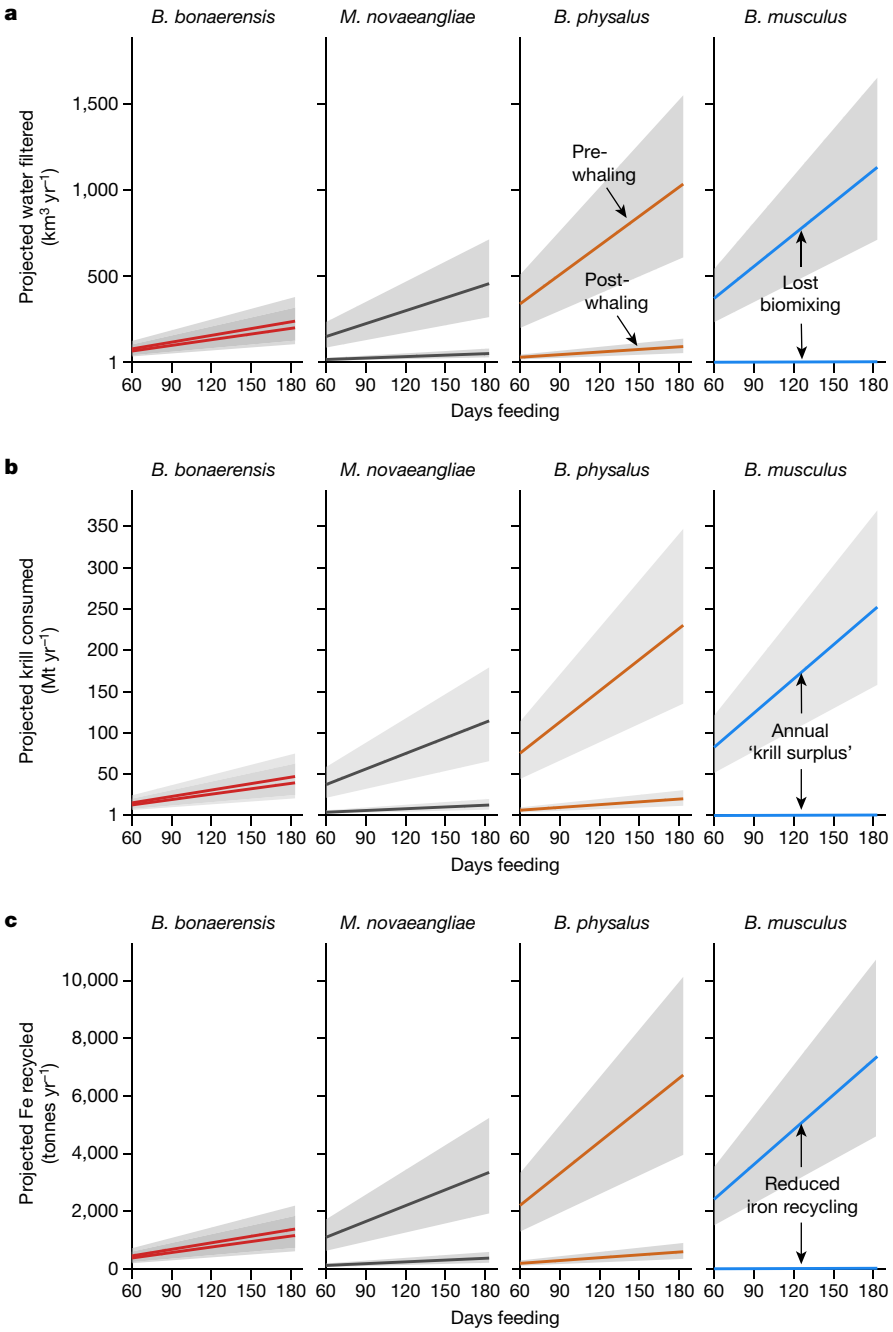

Fig. 4 | Southern Ocean rorqual population-level water filtration, prey consumption and iron recycling. In each panel, the upper lines represent the pre-whaling (1900) Southern Hemisphere populations of Antarctic minke (*B. bonaerensis*), humpback, (*M. novaeangliae*), fin (*B. physalus*) or blue whale (*B. musculus*); the lower lines represent the Southern Hemisphere populations of each species in 2000 (post-whaling). Estimates use a conservative foraging rate for a given number of days feeding (range given, 60–182.5 days; see Methods). Coloured lines represent the median estimate, grey bars are the Q1–Q3 range. **a**, Projected annual water filtration. **b**, Projected annual krill consumption. **c**, The projected loss of fecal iron recycling—for fin and blue whales this represents a >90% decline in the 20th century.

Conclusion

Here we show that prey consumption and ecosystem services provided by baleen whales are likely to be underestimated. For example, data limitations excluded one million mysticetes in our calculations from other populations and species that were hunted during the 19th and 20th centuries. Including these individuals in future analyses may increase our estimates by 20% or more. For the Southern Hemisphere rorqual populations we did consider, the near-complete loss of whale-recycled iron from the largest species (Fig. 4c) suggests a mechanistic explanation of the krill paradox of declining *E. superba* biomass post-whaling[7,35]. The ability for megafauna to engineer a green wave of productivity that sustains both themselves and the ecosystem at large has been reported in terrestrial systems[45], but has yet to be demonstrated in the oceans. Combining the findings presented here with previous research implies that mysticetes not only track green waves[46], but may also amplify these trophic feedback loops.

Large vertebrates, and the ecosystems they support, are in peril[1,16,17]. The collapse of these populations has coincided with steep reductions in ecosystem services they provide[2]. Terrestrial losses have been

mirrored at sea[17], most prominently by 20th-century industrial whaling that reduced global mysticete populations by two thirds, more than twice the total biomass of all wild mammals, terrestrial and marine, on Earth today[47]. Rebuilding defaunated mysticete populations is likely to have significant benefits. For example, restoring the so-called food chain of the giants (that is, diatoms–krill–whales, where each species in this chain is the largest member of its lineage)[13] would positively impact ecosystem structure and function in the Southern Ocean. While some mysticete populations are rebounding[48], climate change and additional anthropogenic stressors (for example, ship strike, entanglement in fishing gear, marine pollution) are inhibiting their recovery globally, thus constraining the ecosystem services that historic populations provided[21]. Encouraging cetacean populations to recover may restore ecosystem function lost in the 20th century and lead to enhanced oceanic productivity, while simultaneously bolstering human wellbeing and planetary health.

Online content

Any methods, additional references, Nature Research reporting summaries, source data, extended data, supplementary information, acknowledgements, peer review information; details of author contributions and competing interests; and statements of data and code availability are available at https://doi.org/10.1038/s41586-021-03991-5.

1. Enquist, B. J., Abraham, A. J., Harfoot, M. B. J., Malhi, Y. & Doughty, C. E. The megabiota are disproportionately important for biosphere functioning. *Nat. Commun.* **11**, 699 (2020).
2. Doughty, C. E. et al. Global nutrient transport in a world of giants. *Proc. Natl Acad. Sci. USA* **113**, 868–873 (2016).
3. Roman, J. & McCarthy, J. J. The whale pump: marine mammals enhance primary productivity in a coastal basin. *PLoS ONE* **5**, e13255 (2010).
4. Barlow, J., Kahru, M. & Mitchell, B. G. Cetacean biomass, prey consumption, and primary production requirements in the California Current ecosystem. *Mar. Ecol. Prog. Ser.* **371**, 285–295 (2008).
5. Fortune, S. M. E., Trites, A. W., Mayo, C. A., Rosen, D. A. S. & Hamilton, P. K. Energetic requirements of North Atlantic right whales and the implications for species recovery. *Mar. Ecol. Prog. Ser.* **478**, 253–272 (2013).
6. Trites, A. W., Christensen, V. & Pauly, D. Competition between fisheries and marine mammals for prey and primary production in the Pacific Ocean. *J. Northwest Atl. Fish. Sci.* **22**, 173–187 (1997).
7. Lavery, T. J. et al. Whales sustain fisheries: blue whales stimulate primary production in the Southern Ocean. *Mar. Mammal Sci.* **30**, 888–904 (2014).
8. Croll, D. A., Kudela, R. & Tershy, B. R. in *Whales, Whaling, and Ocean Ecosystems* (eds. Estes, J. A. et al.) 202–214 (Univ. California Press, 2006).
9. Smith, L. A., Link, J. S., Cadrin, S. X. & Palka, D. L. Consumption by marine mammals on the Northeast U.S. continental shelf. *Ecol. Appl.* **25**, 373–389 (2015).
10. Atkinson, A., Siegel, V., Pakhomov, E. A., Jessopp, M. J. & Loeb, V. A re-appraisal of the total biomass and annual production of Antarctic krill. *Deep. Res. Part I Oceanogr. Res. Pap.* **56**, 727–740 (2009).
11. Pauly, D. & Zeller, D. Catch reconstructions reveal that global marine fisheries catches are higher than reported and declining. *Nat. Commun.* **7**, 10244 (2016).
12. Estes, J. A., Heithaus, M., McCauley, D. J., Rasher, D. B. & Worm, B. Megafaunal Impacts on Structure and Function of Ocean Ecosystems. *Annu. Rev. Environ. Resour.* **41**, 83–116 (2016).
13. Smetacek, V. in *Impacts of Global Warming on Polar Ecosystems* (ed. Duarte, C. M.) 46–80 (Fundacion BBVA, 2008).
14. Wing, S. et al. Seabirds and marine mammals redistribute bioavailable iron in the Southern Ocean. *Mar. Ecol. Prog. Ser.* **510**, 1–13 (2014).
15. Nicol, S. et al. Southern Ocean iron fertilization by baleen whales and Antarctic krill. *Fish Fish.* **11**, 203–209 (2010).
16. Ripple, W. J., Wolf, C., Newsome, T. M., Hoffmann, M. & Wirsing, A. J. Extinction risk is most acute for the world's largest and smallest vertebrates. *Proc. Natl Acad. Sci. USA* **114**, 10678–10683 (2017).
17. McCauley, D. J. et al. Marine defaunation: animal loss in the global ocean. *Science* **347**, 1255641 (2015).
18. Goldbogen, J. A. et al. How baleen whales feed: the biomechanics of engulfment and filtration. *Ann. Rev. Mar. Sci.* **9**, 367–386 (2017).
19. Kleiber, M. *The Fire of Life: An Introduction to Animal Energetics* (Krieger, 1975).
20. Nagy, K. A. Field metabolic rate and body size. *J. Exp. Biol.* **208**, 1621–1625 (2005).
21. Roman, J. et al. Whales as marine ecosystem engineers. *Front. Ecol. Environ.* **12**, 377–385 (2014).
22. Atkinson, A., Siegel, V., Pakhomov, E. & Rothery, P. Long-term decline in krill stock and increase in salps within the Southern Ocean. *Nature* **432**, 100–103 (2004).
23. Lee, C. I. L., Pakhomov, E., Atkinson, A. & Siegel, V. Long-term relationships between the marine environment, krill and salps in the Southern Ocean. *J. Mar. Biol.* **2010**, 410129 (2010).
24. Kahane-Rapport, S. R. & Goldbogen, J. A. Allometric scaling of morphology and engulfment capacity in rorqual whales. *J. Morphol.* **279**, 1256–1268 (2018).
25. Goldbogen, J. A. et al. Why whales are big but not bigger: physiological drivers and ecological limits in the age of ocean giants. *Science* **366**, 1367–1372 (2019).
26. Nickels, C. F., Sala, L. M. & Ohman, M. D. The morphology of euphausiid mandibles used to assess selective predation by blue whales in the southern sector of the California Current System. *J. Crustac. Biol.* **38**, 563–573 (2018).
27. Croll, D. A., Kudela, R. & Tershy, B. R. in *Whales, Whaling, and Ocean Ecosystems* (eds. Estes, J. A. et al.) 202–214 (Univ. California Press, 2006).
28. Fleming, A. H., Clark, C. T., Calambokidis, J. & Barlow, J. Humpback whale diets respond to variance in ocean climate and ecosystem conditions in the California Current. *Glob. Chang. Biol.* **22**, 1214–1224 (2015).
29. Katija, K. Biogenic inputs to ocean mixing. *J. Exp. Biol.* **215**, 1040–1049 (2012).
30. Katija, K., Sherlock, R. E., Sherman, A. D. & Robison, B. H. New technology reveals the role of giant larvaceans in oceanic carbon cycling. *Sci. Adv.* **3**, e1602374 (2017).
31. Riisgård, H. U. On measurement of filtration rates in bivalves — the stony road to reliable data: review and interpretation. *Mar. Ecol. Prog. Ser.* **211**, 275–291 (2001).
32. Drenner, R. W., Mummert, J. R. & O'Brien, W. J. Filter-feeding rates of gizzard shad. *Trans. Am. Fish. Soc.* **111**, 210–215 (1982).
33. Rocha, R. C. Jr, Clapham, P. J. & Ivashchenko, Y. V. Emptying the oceans: a summary of industrial whaling catches in the 20th century. *Mar. Fish. Rev.* **76**, 37–48 (2014).
34. Christensen, L. B. Marine mammal populations: reconstructing historical abundances at the global scale. *Fish. Cent. Res. Reports* **14**, 167 (2006).
35. Laws, R. M. Seals and whales of the Southern Ocean. *Philos. Trans. R. Soc. B Biol. Sci.* **279**, 81–96 (1977).
36. Myers, R. A. & Worm, B. Rapid worldwide depletion of predatory fish communities. *Nature* **423**, 280–283 (2003).
37. Trathan, P. N., Ratcliffe, N. & Masden, E. A. Ecological drivers of change at South Georgia: the krill surplus, or climate variability. *Ecography* **35**, 983–993 (2012).
38. Dunn, M. J. et al. Population size and decadal trends of three penguin species nesting at Signy Island, South Orkney Islands. *PLoS ONE* **11**, e0164025 (2016).
39. Falkowski, P. G., Barber, R. T. & Smetacek, V. Biogeochemical controls and feedbacks on ocean primary production. *Science* **281**, 200–206 (1998).
40. Ratnarajah, L. et al. A preliminary model of iron fertilisation by baleen whales and Antarctic krill in the Southern Ocean: sensitivity of primary productivity estimates to parameter uncertainty. *Ecol. Modell.* **320**, 203–212 (2016).
41. Willis, J. Whales maintained a high abundance of krill; both are ecosystem engineers in the Southern Ocean. *Mar. Ecol. Prog. Ser.* **513**, 51–69 (2014).
42. Gerber, L. R., Morissette, L., Kaschner, K. & Pauly, D. Should whales be culled to increase fishery yield? *Science* **323**, 880–881 (2009).
43. Ruzicka, J. J., Steele, J. H., Ballerini, T., Gaichas, S. K. & Ainley, D. G. Dividing up the pie: whales, fish, and humans as competitors. *Prog. Oceanogr.* **116**, 207–219 (2013).
44. Arrigo, K. R., van Dijken, G. L. & Bushinsky, S. Primary production in the Southern Ocean, 1997-2006. *J. Geophys. Res. Ocean.* **113**, C08004 (2008).
45. Geremia, C. et al. Migrating bison engineer the green wave. *Proc. Natl Acad. Sci. USA* **116**, 25707–25713 (2019).
46. Abrahms, B. et al. Memory and resource tracking drive blue whale migrations. *Proc. Natl Acad. Sci. USA* **116**, 5582–5587 (2019).
47. Bar-on, Y. M., Phillips, R. & Milo, R. The biomass distribution on Earth. *Proc. Natl Acad. Sci. USA* **115**, 6506–6511 (2018).
48. Pallin, L. J. et al. High pregnancy rates in humpback whales (*Megaptera novaeangliae*) around the Western Antarctic Peninsula, evidence of a rapidly growing population. *R. Soc. Open Sci.* **5**, 180017 (2018).
49. Aksnes, D. L. & Ohman, M. D. Multi-decadal shoaling of the euphotic zone in the southern sector of the California Current System. Limnol. Oceanogr. 54, 1272–1281 (2009).

Methods

Prior estimation of prey consumption

Estimates of mysticete prey consumption (that is, mass of prey consumed per day) date to the height of industrial whaling[50], and have been debated in the decades since that time[4,9,27,51–54]. Previous estimates of daily prey consumption derive from (1) extracting and weighing stomach contents from kills[55,56], (2) bioenergetic models reliant on assumptions of metabolic rates and digestive assimilation efficiencies[4,6,57,58], or a combination of the two approaches[59–62].

Studies from industrial whaling operations extracted and weighed prey contents from the stomach (forestomach, fundic and pyloric chambers) or less commonly from the entire gastrointestinal tract[63] of whales killed throughout the day[59,64–66]. These studies were often restricted to specific points in the season[63], which could bias estimated prey consumption. Some have attempted to measure forestomach volume by filling the chamber with water or gas, but noted that the elasticity of the stomach declines after death, and combined with imperfect sealing and filling of the stomach compartments, creates minimum estimates of maximum fill volumes[63]. For example, fin whales feeding near Iceland had an estimated stomach capacity of 500–600 kg, with a projected daily consumption rate of 677–1,377 kg d^{-1}, corresponding to 1–3% of body weight per day[67].

Bioenergetic models employing metabolic theory have also been used to estimate mysticete prey consumption. However, mysticete metabolic rates were not directly measured, and instead extrapolated from measurements on captive odontocetes, further parameterized with mysticete breathing rates[19,68]. The two most commonly used metabolic equations to evaluate the daily biomass consumed (in kg) solve for the 'daily ration' (R)[4,53]. One of these equations is:

$$R = \frac{\gamma(\mathrm{BMR})}{0.8(3{,}900Z + 5{,}400(1 - Z))} \quad (1)$$

Where the basal metabolic rate (BMR) takes the form BMR = $293.1M^{0.75}$, where M is the mass of the animal in kilograms[19]. BMR is multiplied by the constant γ to estimate field metabolic rate (FMR, or the average daily metabolic rate (ADMR)[4]). The conversion factor from BMR to FMR, γ, is typically assumed to be between 2–5 (ref. [53]), and 2.5 and 3 are most commonly used[3,4,27,57]. The FMR is divided by an estimate of the daily energy intake, which uses average prey energy densities of 3,900 kJ kg^{-1} and 5,450 kJ kg^{-1} for krill and forage fish, respectively, adjusted for assimilation efficiency[51]. Diet composition (Z) values, a proportion ranging from 0 to 1, were obtained from ref. [69].

The majority of studies of mysticete prey consumption have used the metabolic scaling equation:

$$R = \alpha M^{\beta} \quad (2)$$

Where M is the mass of the animal in kg, α is a constant and β is a metabolic scaling exponent, typically in the range of 0.6–1.0 (Extended Data Table 3). For an overview of these methods see ref. [70]. These two equations assume mysticetes ingest an equal amount of prey each day throughout the year (that is, R is constant). However, mysticetes exhibit a feast–fast annual phenology with a majority of yearly ingestion occurring in productive regions at mid- to high latitudes during a six-month feeding season. It has been estimated that roughly four fifths (83%) of the whale's annual caloric intake occurs during 90–120 days of high-intensity feeding during this period[4,51,53]. Therefore, estimates of mean daily consumption (MDC in kg d^{-1}) during the foraging season using estimates of R from equation (1) or (2) would take the form:

$$\mathrm{MDC} = \frac{0.83(365R)}{D_{\max}} \quad (3)$$

Where $D_{\max}$ is the number of days feeding within a foraging season.

These prey consumption estimates (Extended Data Fig. 1) are based on predicted mass-specific metabolic rates for mysticetes, which are low compared to other eutherians. However, numerous aspects of mysticete life history and ecology correlate with elevated metabolic rates including their aquatic lifestyle[71], rapid pace of reproduction[51,72], muscular physiology[73] and energetically demanding feeding strategies[18].

Tagging methods

Tag specifications. Short-duration tags (<24 h) used in this study were DTAG (digital acoustic recording tags; www.soundtags.org/dtags) and CATS (Customized Animal Tracking Solutions; www.cats.is) tags attached via suction cups. DTAGs were equipped with the following sensors: pressure transducer (50 Hz), tri-axial accelerometers (250 Hz), magnetometers (50 Hz) and hydrophone. CATS camera tags integrate high-definition video with tri-axial accelerometers (400 Hz) and gyroscopes (50 Hz); magnetometers (50 Hz), pressure (10 Hz), and temperature sensors (10 Hz); and light and GPS sensors (both 10 Hz). Videos were recorded in 1,280 × 720 p or 1,920 × 1,080 p resolution at between 25 and 30 frames per second, while audio was recorded with a single embedded hydrophone at a 22.5 kHz sampling rate with 16-bit resolution.

Medium-duration (multi-day) tags used in this study were Wildlife Computers TDR10-F (https://wildlifecomputers.com/our-tags/tdr/tdr10/) and Acousonde acoustic (http://www.acousonde.com) tags. These tags were modified to take a plate with darts and a satellite transmitter and were attached with 3–4 stainless steel darts 4–6 cm long. Both tag types included depth and orientation sensors as well as Fastloc GPS. More details on these tags can be found in[74,75].

Deployment. Tags were deployed from 6 m rigid hull inflatable boats using a 6 m carbon-fibre pole. Tags were attached to the animal with four suction cups, detached after suction failed, floated to the surface, and were recovered via VHF telemetry. Deployment duration averaged 10 h. Tagging operations were performed under NMFS permits 16111, 14809, 19116, 21678, 20430, and NMS permits MULTI-2017-007 and MULTI-2019-009, in accordance with Stanford University IACUC (#30123) and under the South African Department of Forestry, Fisheries and Environment (DFFE): RES2018/63 and RES2019/57 in accordance with the Research Ethics Committee (Animal) of Nelson Mandela University A18-SCI-ICMR-001. A subset of tag deployments used in this paper have been previously published in refs. [25,74–79,96]. Additional details on the tags and tagging procedures can be found in refs. [25,67,75,76,79,96].

Lunge detection methods

We included deployments containing at least one lunge—to conservatively classify that day as a feeding day—and that lasted more than one hour to minimize tagging effects. All data were decimated to 10 Hz before analysis for CATS tags or 5 Hz for DTAGs. Tag data was rotated from the tag's frame of reference (subject to tag placement) to the whale's reference frame (x, y and z oriented longitudinally, laterally and dorso-ventrally, respectively) using periods of known orientation. Animal orientation (pitch, roll and heading) was calculated using custom-written MATLAB scripts[76,80]. Individual speed was determined using the amplitude of tag vibrations[81]. To identify lunge feeding events, we used kinematic signatures derived from the tag data. These include intense fluking leading to rapid acceleration to ≥4 m s^{-1} followed immediately a rapid deceleration coinciding with mouth opening[76], as well as abrupt changes in pitch and roll characteristic of lunge feeding[76,82]. When possible, we confirmed feeding events with concurrent video. Differences in feeding rates (for example, within the same species lower lunge rates for fish-feeding individuals as compared to krill-feeding individuals, see Fig. 2b and Extended Data Fig. 5a), behaviour, and kinematics[18,76] allowed us to discriminate between prey types for populations that feed on both fish and krill (for example, humpback and fin whales). For a subset of the deployments, prey type was confirmed with

video (Extended Data Table 4). For roughly half of the deployments, acoustically detected krill patches were also measured proximal to foraging whales with SIMRAD EK 60 and EK80 multi-frequency echosounders (Extended Data Table 4, see the 'Prey methods' section). We detected lunges manually to maximize accuracy. Lunges were identified from the raw data and stored with concurrent kinematic data as well as the date and time.

Prey methods

Krill. The majority of whales in this study were rorqual whales either presumed or confirmed to be feeding on krill (207/321 deployments; Extended Data Table 1). Krill data were collected using a multi-frequency (38 and 120 kHz), split-beam fisheries acoustic system (Simrad EK60s or EK80s) and processed for ref. [25]. Density and biomass were converted from acoustic units using previously published target strength–length (TS–L) relationships and krill size measurements[25,83,84].

In the ENP, krill patches near foraging whales were assumed to primarily be composed of *T. spinifera* given the published prey preferences of blue whales[26]. In the West Antarctic Peninsula (WAP), krill patches near foraging whales were assumed to be composed of *E. superba*[85]. We examined the distribution of prey available to lunge-feeding whales in an environment as in ref. [25]. We used Echoview to linearly average S_v within acoustic cells the size of an average whale gulp (henceforth, S_{v_gulp}). This gulp-sized water volume of rorqual whales represents the finest possible scale of decision-making by a foraging whale (see ref. [25]. for species-specific S_{v_gulp} cell sizes). For each krill patch in a region of interest, we summarized the distribution of biomasses likely to be experienced by a foraging whale by calculating the log mean (that is, the geomean) and standard deviation of S_{v_gulp} within each measured krill patch.

To quantify the krill consumption per lunge-feeding event, we created a lognormal distribution of krill biomass (ρ_p)—unique for each rorqual species of interest (see 'Prey biomass density' column in Extended Data Table 1)—using the geomean biomass and geometric standard deviation multiplied by the species-specific engulfment capacity (V_e; see the 'Drone/engulfment capacity methods' section) to generate species-specific prey consumption estimates. Daily krill consumption estimates (P_C krill; see the 'Daily prey consumption methods for rorquals' section for more details) were calculated combining lunge-specific consumption estimates with the daily lunge rate (r_f daily). In the ENP, we also included estimates that were generated with previously published methods[83,84,86] that used *E. superba* TS–L equations to produce biomass estimates for ENP krill from which we generated a lower-bound estimate of prey consumption in this ecosystem (Extended Data Fig. 5d).

Antarctic blue and fin whale prey consumption was estimated using feeding rates from ENP blue and fin whales with krill densities calculated from humpback whale foraging grounds in the WAP as there are no available data (high-resolution tag data nor krill acoustic data) for Antarctic fin and blue whales. This is a conservative method of deriving prey consumption for Antarctic blue and fin whales. A different approach, the energy conversion method, converts the estimated amount of energy consumed per day by an ENP whale into a biomass of *E. superba* (using an average energy density of 4,575 kJ kg^{-1} *E. superba*[25]). This approach produces higher prey consumption estimates than the feeding rate approach. For example, using the feeding rate approach we estimated the median daily consumption for an Antarctic blue whale (*B. m. intermedia*) to be 4.2 tonnes d^{-1} (Q1–Q3 range, 2.7–6.1 tonnes d^{-1}) of *E. superba*, whereas the energy conversion approach suggests a median daily consumption of 12.6 tonnes d^{-1} (Q1–Q3 range, 8.3–17.4 tonnes d^{-1}) tof *E. superba*. Due to a lack of energy density data on krill collected near foraging whales, we used the feeding rate approach—the more conservative of the two methodsrecognizing this may be an underestimate.

For the ENP, we calculated the geometric mean of densities between our two prey mapping sites (Monterey Bay National Marine Sanctuary and the Southern California Bight) to generate an ecosystem average (Extended Data Table 1). Finally, in our calculations we assumed maximal engulfment and 100% capture of krill, as has been previously published[25,87]. We recognize this may be an overestimate, but we have no evidence to suggest a lower capture rate. This is based on extensive tag-video observations—where we have not observed krill escape behaviour—as well as at least a fivefold difference between a lunging whale[76,88] and maximum krill escape speeds[89]. Suction created by mouth opening in rorqual whales could also maximize capture rate[90], and rorqual rolling behaviours could increase the quantity of prey engulfed within a given volume[91,92].

Fish (anchovy). We modelled whales' lunge-specific catch percentage of fish based on calculated approach parameters from[87]. We used the alpha-inhibitory model[87] to calculate a mean of 37.5% and standard deviation of 24.3% catch with every lunge. Detailed methods to produce this catch percentage parameters are fully described in ref. [87]. Our upper estimate of prey consumption by fish-feeding rorquals assumed that fish schools were at least as large as the whale's engulfment capacity (Extended Data Table 1, Extended Data Fig. 5c). The lower fish-consumption estimate assumes smaller fish schools that are 29% of the size of the engulfment volume. These are similar metrics used by ref. [87]. (Extended Data Table 1, Extended Data Fig. 5c).

Escape-engulfment data generated for ENP anchovy-feeding humpback whales described above were used to generate estimates for fish-feeding humpback whales at Stellwagen Bank, and Bryde's whales off South Africa. We only considered feeding events that occurred in the water column; bottom-feeding from humpback whales in Stellwagen Bank National Marine Sanctuary were excluded due to the complexity of, and lack of detailed information on, this feeding behaviour.

For the density of fish in a school we used a value of 7.8 kg m^{-3} of fish based on published length–weight relationships from ref. [93], a school packing density of one body length cubed per fish[94], and a representative fish length of 12 cm (ref. [87]). These simplifying assumptions do not reflect the natural variability in fish schools; however, there are not robust school density estimates in the patches of forage fish whales have been observed to feed on.

Copepods. Balaenid whales are thought to feed almost exclusively on copepods. For bowhead whales, copepod (*Calanus* spp.) biomass densities (ρ_p) ranged from 1–10 g m^{-3} in regions where bowhead whales were foraging[95,96], but were higher—170 g m^{-3}—in regions where North Atlantic right whales were foraging[97,98]. This difference is believed to be due to the right whale's smaller gape and higher swimming drag that necessitate more efficient feeding on higher density prey patches[97,98]. As a result, we used the average copepod density of the range provided for bowhead whales (6 g m^{-3}), and 170 g m^{-3} for North Atlantic right whales, recognizing that both values may be underestimates.

Drone/engulfment capacity methods

Photographs were collected using unoccupied aircraft systems (UAS, or drones) to measure the total length of a subset of the tagged rorqual whales. Four different UAS aircraft were used throughout the course of the study: two quadcopters (DJI Phantom 4; DJI Phantom 4 adv) and two hexacopters (LemHex 44; Freefly Alta 6). Each aircraft contained a barometric altimeter, while both hexacopters also contained a laser altimeter (LightWare SF11-C LIDAR). Due to the absence of a laser altimeter, both quadcopters were flown at heights sufficient to minimize errors (approximately above 50 m); an accurate altimeter reading was confirmed during each flight using the known length of the boat (50 m (ref. [99])). Nadir photos were taken as the whales surfaced and body lengths were measured in pixels and converted to metres using MorphoMetriX photogrammetry software[100] from the altitude of the UAS, the focal length of the camera, and the pixel size[99–102]. When possible, multiple photos of the same whale were taken and the largest credible measurement was used[102]. We applied the UAS-based length

estimates to species-specific allometric equations to estimate buccal cavity volumes. The general equation is:

$$V_e = L_B^{slope} \times 10^{intercept} \quad (4)$$

Where V_e corresponds to the engulfment capacity in m^3 and L_B is the drone-measured body length in metres. Each species of rorqual has unique slope and intercept parameters. More details about this method can be found in ref. [24].

Rorqual feeding rate methods

The distribution of daily rorqual feeding rates was estimated separately for day, twilight and night (phases). We segmented each deployment's phases according to astronomical definitions of day (sun angle ≥0°), twilight (0° > sun angle ≥ −18°), and night (sun angle <−18°) and recorded the duration (in hours) and lunge frequency (in lunges per hour). Sun angle was calculated with the oce package[103] in R (v3.6). To generate an empirical distribution of day feeding rates by species and phase, we sampled deployments' lunge frequency with replacement weighted by duration, validated with multi-tag deployments (see next section). Unlike day and twilight, all deployments were weighted equally to derive night-time feeding estimates because feeding rates are low at night in temperate feeding grounds (for example, ENP) and there are few hours of astronomical night in polar regions (for example, WAP) during the feeding season.

Feeding rate validation

We used multi-day tag deployments (n = 16 blue whale deployments, n = 6 fin whale deployments, 126.4 days total, mean 5.7 days) to test if sub-daily deployments produce biased daily-feeding estimates. For each full day of multi-day deployments, we subsampled 1- to 10-h periods and compared the hourly lunge-rate of the subsample to the full day. Weighting the deployments strictly by duration over-emphasizes longer deployments; therefore, we used a nonlinear asymptotic regression to predict the mean absolute error of hourly lunge rate with respect to sub-daily deployment duration.

We generated a distribution of daytime hourly feeding rates using the full sub-daily dataset. We had greater confidence in the estimates from longer deployments and weighted the probabilities according to the inverse of the error prediction found using the multi-day deployments. Our data-informed function weighted all deployments ≥10 h equally and everything shorter by the inverse of the predicted error (Extended Data Fig. 6).

Daily prey consumption methods for rorquals

We estimated rorqual and balaenid prey consumption using separate methods because of differences between discrete (rorqual) and continuous (balaenid) feeding events.

For rorquals, daily prey consumption was estimated as:

$$P_c = \sum_{phase} r_f V_e \rho_p t \quad (5)$$

Where P_c is prey consumption (kg d^{-1}), phase is daylight or night, r_f is feeding rate (lunges hr^{-1}), V_e is the engulfment volume (m^3), ρ_p is biomass density (kg m^{-3}), and t is the duration of each phase. A distribution for P_c was generated by sampling r_f (see section Rorqual feeding rate methods), V_e (see the 'Drone/engulfment capacity methods' section), and ρ_p (see section 'Prey methods') 1,000 times with replacement for each day of the feeding season (121 days with varying daylight/night dependent on latitude and hemisphere) for each species' population in each ecosystem.

For energetic values we used 6,000 kJ kg^{-1} for forage fish according to ref. [104], 4,575 kJ kg^{-1} for Antarctic krill (*E. superba*) according to ref. [25], 3,628 kJ kg^{-1} for non-Antarctic krill derived from a weighted average consisting of 80% *T. spinifera* (3,800 kJ kg^{-1} from ref. [105]), and 20% *E. pacifica* (2,940 kJ kg^{-1} from ref. [105]), representing the strong preference of *T. spinifera* by krill-feeding rorquals in the California Current Ecosystem, where all tagged ENP whales in this study were feeding[26] (Extended Data Fig. 2).

Balaenid water filtration and prey estimation methods

We calculated the volume flow rate Q through the oral cavity in $m^3\ s^{-1}$ using methods outlined in ref. [106] (Extended Data Fig. 4a). Data for the morphometrics (anterior and posterior opening area, AO and PO) and kinematics (swimming speed during feeding, V) were taken from figure 9 of ref. [98]. There is no posterior opening measurement for the North Atlantic right whale (*Eu. glacialis*), so we estimated the opening area to be one third the area of the anterior opening based upon the measurements of AO and PO for the bowhead whale (*Ba. mysticetus*). We then used the following equations to first calculate the pressure differential across the oral cavity (ΔP) and then calculate the Q:

$$\Delta P = \frac{\rho V^2}{2(1 - \frac{AO^2}{PO^2})} \quad (6)$$

$$Q = C_o \pi r^2 \sqrt{2\Delta P/\rho} \quad (7)$$

Where ρ is the density of seawater (1025 kg m^{-3}), C_o is the dimensionless orifice coefficient (estimated at 0.6), and r is the radius of the anterior opening.

Using accelerometer tag deployments from bowhead whales (n = 6) and North Atlantic right whales (n = 23), we separated out U-shaped foraging dives (n = 343) from non-foraging V-shaped dives using the parameters laid out in ref. [96] and, for foraging dives, further separated the bottom phase from the descent and ascent periods. The bottom phase started at the first inflection point that was greater than 80% of the deepest depth for that dive where the animal switched from a downward pitch to an upward pitch and the bottom phase ended at the last such inflection point. Balaenid whales are thought to fluke with their mouth open[107], so we used periods of continuous fluking during the bottom phase of a dive as a proxy for feeding in lieu of cameras to directly see the behaviour. We determined periods of fluking versus non-fluking using a series of threshold values described in ref. [77].

We estimated daily balaenid prey consumption as:

$$P_c = f_f Q \rho_p t_d \quad (8)$$

Where f_f is the percent time feeding, Q is the volume flow rate, ρ_p is biomass density (kg m^{-3}), and t_d is duration of daylight (s). Conservatively, we assumed balaenids only feed during the day. f_f was calculated as the fraction of time spent fluking at the bottom of dives relative to the entire duration. A distribution of P_c for balaenids was generated by sampling f_f from tag deployments with replacement weighted by deployment duration (Extended Data Fig. 4). We conducted energetic calculations for balaenids using an energy density of 6,295 kJ kg^{-1} for the copepod *Calanus finmarchicus*[108], a common diet item for both bowhead and North Atlantic right whale (Extended Data Fig. 4e).

Annual and population-level projections

To project annual prey consumption rates, we multiplied our daily prey consumption values (P_c) from 60 to 182.5 because this encompasses the full range of total number of possible days feeding for baleen whales[51,56,109,110]. Even so, we consider our estimates conservative because we do not account for any foraging occurring outside this season, despite the assumption that ~17% of the annual prey consumption occurs during the period of non-intensive feeding[4,51]. To project the annual water filtration and prey consumption of mysticetes we multiplied annual individual values by abundance estimates from 1900 (pre-whaling; 'historic') and 2000 (post-whaling 'current')[34]. For Southern Ocean fin and blue whales, we informed our projections using feeding rates from Northern Hemisphere individuals coupled with *E. superba* densities measured in the Southern Ocean.

To estimate the total circumpolar biomass of *E. superba* in 2000 to compare to mysticete prey requirements, we used the same methods in ref. [10], but with an updated estimate of 60.3 Mt of *E. superba* in the CCAMLR synoptic survey area[111]. This region contains ~28% of the total biomass of *E. superba*. Dividing the 60.3 Mt from this region by 0.28 reveals an estimate of 215.36 Mt as the total circumpolar biomass of *E. superba* in 2000. The total biomass of *E. superba* in 1900 is thought to be greater, but how much greater is unknown. The largest decline of *E. superba* in the 20th century was observed in the Southwest Atlantic Sector (the region containing the APP)[22,112], which was also the region where the most whales were killed.

Iron recycling and primary production

To estimate the amount of iron recycled by Southern Ocean populations of rorqual whales, we used values from the published literature on baleen whale assimilation efficiencies and fecal iron content. The exact quantity of egesta that whales produce is unknown; however, there is a growing body of literature on the nutrient content of mysticete feces. In particular, we used published concentrations of iron from Southern Ocean rorquals[15,113]. The equation for iron egested (recycled) is:

$$\mathrm{Fe}_{\mathrm{recycled}} = \frac{P_c}{4}\mathrm{Fe}_{\mathrm{conc}} \quad (9)$$

Where P_c is prey mass consumed; dividing the total amount of feces produced by four converts from wet weight to dry weight[114]. $\mathrm{Fe}_{\mathrm{conc}}$ is the concentration of iron in mysticete feces by dry weight. To incorporate uncertainty in our calculations, we sampled from a distribution of possible values for $\mathrm{Fe}_{\mathrm{conc}}$ (normal distribution, 146 ± 135 mg kg^{-1} mean and standard deviation[113] cutoff at zero to exclude negative values) from previously published estimates from baleen whales. Iron-retention and egestion rates by mysticetes have not been measured directly, though Fe:C ratios in whale and krill tissues as compared to their fecal material suggests that foraging whales concentrate carbon and egest a majority of ingested iron[113].

We further validated the total quantity of iron recycled (egested) by separately estimating the total iron reservoir in krill consumed by whales and assuming that 80% of ingested iron is egested by adult mammals (measured in pigs and humans[115]). We compared our results of iron egested with the calculation described above and found these numbers to be comparable. For example, the approximate iron reservoir in 400 Mt *E. superba* is 1.6×10^4 t, whereas we found historic populations of Antarctic minke, humpback, fin and blue whales that we estimate to have consumed 428 Mt *E. superba* yr^{-1} to have recycled $1.2{\times}10^4$ tonnes yr^{-1}.

Using the assumptions of Ratnarajah et al.[116] that (1) 50% of this iron deposited by whales remains in the photic zone, and (2) 50% of that iron is bioavailable to phytoplankton, implies that 3×10^3 tonnes yr^{-1} of whale-recycled iron was incorporated by phytoplankton across the Southern Ocean pre-whaling (Extended Data Table 2). The average iron-carbon ratio of Southern Ocean diatoms is 3 µmol Fe: mol C[117–119]; thus, whale-mediated recycling of 3×10^3 tonnes iron yr^{-1} may correspond to a NPP increase of 215 TgC yr^{-1} (see Extended Data Table 2 for calculations). This represents an 11% enhancement of annual NPP (range, 1–75%; see Extended Data Table 2) compared to Southern Ocean NPP from the end of the 20th century[44]. These percentages were probably greater at finer spatial scales. For example, the majority of mysticetes harvested in the 20th century were taken from the Scotia and Weddell Seas. This section of the Southern Ocean had an estimated NPP of 477 TgC yr^{-1} at the end of the 20th century[44]. If half of all iron recycled by whales occurred there, this may have boosted NPP in the Scotia and Weddell Seas by 22.5% as compared to present. Despite simplifying assumptions, our calculations define a boundary on the role of large cetaceans in stimulating primary production.

Reporting summary

Further information on research design is available in the Nature Research Reporting Summary linked to this paper.

Data availability

Code to reproduce the figures and analyses in this paper are available at: https://github.com/mssavoca/prey_consumption_paper; all data and code are available on GitHub.

50. Krough, A. The physiology of the blue whale. *Nature* **133**, 635–637 (1934).
51. Lockyer, C. in *Mammals in the Seas: Large Cetaceans* (eds. Clarke, J. G., Goodman, J. & Soave, G. A.) 379–487 (FAO, 1981).
52. Tamura, T. & Ohsumi, S. Regional assessments of prey consumption by marine cetaceans in the world. *International Whaling Comission Scientific Report* (2000); https://doi.org/10.1079/9780851996332.0143
53. Leaper, R. & Lavigne, D. How much do large whales eat? *J. Cetacean Res. Manag.* **9**, 179–188 (2007).
54. Klumov, S. K. Food and helminth fauna of whalebone whales (Mystacoceti) in the main whaling regions of the world ocean. *Tr. Instituta Okeanol.* **71**, 94–194 (1963).
55. Sigurjónsson, J. & Víkingsson, G. A. Estimation of food consumption by cetaceans in Icelandic and adjacent waters. *J. Northw. Atl. Fish. Sci* **22**, 271–287 (1997).
56. Tamura, T. & Konishi, K. Food habit and prey consumption of Antarctic minke whale Balaenoptera bonaerensis in JARPA research area. *Inst. Cetacean Res. Rep.* SC/D06/J18 (2006).
57. Kenney, R. D., Scott, G. P., Thompson, T. J. & Winn, H. E. Estimates of prey consumption and trophic impacts of cetaceans in the USA northeast continental shelf ecosystem. *J. Northwest Atl. Fish. Sci.* **22**, 155–171 (1997).
58. Innes, B. Y. S., Lavigne, D. M., Earle, W. M. & Kovacs, K. M. Feeding rates of seals and whales. *J. Anim. Ecol.* **56**, 115–130 (1987).
59. Tamura, T. & Konishi, K. Prey composition and consumption rate by Antarctic minke whales based on JARPA and JARPAII data. *Inst. Cetacean Res. Rep.* SC/F14/J15 (2014).
60. Tamura, T. Preliminary analyses on prey consumption by fin whales based on JARPAII data. *Inst. Cetacean Res. Rep.* SC/F14/J16 (2014).
61. Tamura, T., Konishi, K. & Isoda, T. Updated estimation of prey consumption by common minke, Bryde's and sei whales in the western North Pacific. *Inst. Cetacean Res. Rep*. SC/F16/JR15 (2016).
62. Lockyer, C. All creatures great and smaller: a study in cetacean life history energetics. *J. Mar. Biol. Assoc. UK* **87**, 1035–1045 (2007).
63. Víkingsson, G. A. Feeding of fin whales (*Balaenoptera physalus*) off Iceland - diurnal and seasonal variation and possible rates. *J. Northwest Atl. Fish. Sci.* **22**, 77–89 (1997).
64. Ichii, T. & Kato, H. Food and daily food consumption of southern minke whales in the Antarctic (Balaenoptera acutorostrata). *Polar Biol.* **11**, 479–487 (1991).
65. Tamura, T. & Konishi, K. Feeding habits and prey consumption of Antarctic minke whale (*Balaenoptera bonaerensis*) in the Southern Ocean. *J. Northwest Atl. Fish. Sci.* **42**, 13–25 (2009).
66. Lockyer, C. Body fat condition in northeast Atlantic fin whales, *Balaenoptera physalus*, and its relationship with reproduction and food resource. *Can. J. Fish. Aquat. Sci.* **43**, 142–147 (1986).
67. Goldbogen, J. A. et al. Using digital tags with integrated video and inertial sensors to study moving morphology and associated function in large aquatic vertebrates. *Anat. Rec.* **300**, 1935–1941 (2017).
68. Sumich, J. L. Swimming velocities, breathing patterns, and estimated costs of locomotion in migrating gray whales, *Eschrichtius robustus*. *Can. J. Zool.* **61**, 647–652 (1983).
69. Pauly, D., Trites, A. W., Capuli, E. & Christensen, V. Diet composition and trophic levels of marine mammals. *ICES J. Mar. Sci.* **55**, 467–481 (1998).
70. White, C. R. & Kearney, M. R. Metabolic scaling in animals: methods, empirical results, and theoretical explanations. *Compr. Physiol.* **4**, 231–256 (2014).
71. Schmitz, O. J. & Lavigne, D. M. Intrinsic rate of increase, body size, and specific metabolic rate in marine mammals. *Oecologia* **62**, 305–309 (1984).
72. Nagy, K. A., Girard, I. A. & Brown, T. K. Energetics of free-ranging mammals, reptiles, and birds. *Annu. Rev. Nutr.* **19**, 247–277 (1999).
73. Rivero, J.-L. L. Locomotor muscle fibre heterogeneity and metabolism in the fastest large-bodied rorqual: the fin whale (*Balaenoptera physalus*). *J. Exp. Biol.* **221**, jeb177758 (2018).
74. Friedlaender, A. S. et al. The advantages of diving deep: Fin whales quadruple their energy intake when targeting deep krill patches. *Funct. Ecol.* **34**, 497–506 (2019).
75. Calambokidis, J. et al. Differential vulnerability to ship strikes between day and night for blue, fin, and humpback whales based on dive and movement data from medium duration archival tags. *Front. Mar. Sci.* **6**, 543 (2019).
76. Cade, D. E., Friedlaender, A. S., Calambokidis, J. & Goldbogen, J. A. Kinematic diversity in rorqual whale feeding mechanisms. *Curr. Biol.* **26**, 2617–2624 (2016).
77. Gough, W. T. et al. Scaling of swimming performance in baleen whales. *J. Exp. Biol.* **222**, jeb204172 (2019).
78. Parks, S. E., Warren, J. D., Stamieszkin, K., Mayo, C. A. & Wiley, D. Dangerous dining: Surface foraging of North Atlantic right whales increases risk of vessel collisions. *Biol. Lett.* **8**, 57–60 (2012).
79. Nowacek, D. P. et al. Buoyant balaenids: the ups and downs of buoyancy in right whales. *Proc. R. Soc. B Biol. Sci.* **268**, 1811–1816 (2001).
80. Johnson, M. P. & Tyack, P. L. A digital acoustic recording tag for measuring the response of wild marine mammals to sound. *IEEE J. Ocean. Eng.* **28**, 3–12 (2003).

81. Cade, D. E., Barr, K. R., Calambokidis, J., Friedlaender, A. S. & Goldbogen, J. A. Determining forward speed from accelerometer jiggle in aquatic environments. *J. Exp. Biol.* **221**, 170449 (2018).
82. Goldbogen, J. A. et al. Integrative approaches to the study of baleen whale diving behavior, feeding performance, and foraging ecology. *Bioscience* **63**, 90–100 (2013).
83. Hazen, E. L., Friedlaender, A. S. & Goldbogen, J. A. Blue whales (Balaenoptera musculus) optimize foraging efficiency by balancing oxygen use and energy gain as a function of prey density. *Sci. Adv.* **1**, e1500469 (2015).
84. Cade, D. E. et al. Predator-scale spatial analysis of intra-patch prey distribution reveals the energetic drivers of rorqual whale super group formation. *Fucntional Ecol.* **35**, 894–908 (2021).
85. Nowacek, D. P. et al. Super-aggregations of krill and humpback whales in Wilhelmina bay, Antarctic Peninsula. *PLoS ONE* **6**, 2–6 (2011).
86. Goldbogen, J. A. et al. Prey density and distribution drive the three-dimensional foraging strategies of the largest filter feeder. *Funct. Ecol.* **29**, 951–961 (2015).
87. Cade, D. E., Carey, N., Domenici, P., Potvin, J. & Goldbogen, J. A. Predator-informed looming stimulus experiments reveal how large filter feeding whales capture highly maneuverable forage fish. *Proc. Natl Acad. Sci. USA* **117**, 472–478 (2020).
88. Goldbogen, J. A. et al. Mechanics, hydrodynamics and energetics of blue whale lunge feeding: efficiency dependence on krill density. *J. Exp. Biol.* **214**, 131–146 (2011).
89. Hamner, W. M. Aspects of schooling in Euphausia superba. *J. Crustac. Biol.* **4**, 67–74 (1984).
90. Potvin, J., Goldbogen, J. A. & Shadwick, R. E. Passive versus active engulfment: verdict from trajectory simulations of lunge-feeding fin whales *Balaenoptera physalus*. *J. R. Soc. Interface* **6**, 1005–1025 (2009).
91. Potvin, J., Goldbogen, J. A. & Shadwick, R. E. Scaling of lunge feeding in rorqual whales: an integrated model of engulfment duration. *J. Theor. Biol.* **267**, 437–453 (2010).
92. Goldbogen, J. A. et al. Underwater acrobatics by the world's largest predator: 360° rolling manoeuvres by lunge-feeding blue whales. *Biol. Lett.* **9**, 20120986 (2013).
93. Rodriguez-Romero, J., Palacios-Salgado, D. S., Lopez-Martinez, J., Vazquez, S. H. & Velazquez-Abunader, J. I. The length – weight relationship parameters of demersal fish species off the western coast of Baja California Sur, Mexico. *J. Appl. Ichthology* **25**, 114–116 (2009).
94. Pitcher, T. J. & Partridge, B. L. Fish school density and volume. *Mar. Biol.* **394**, 383–394 (1979).
95. Laidre, K. L., Heide-Jørgensen, M. P. & Nielsen, T. G. Role of the bowhead whale as a predator in West Greenland. *Mar. Ecol. Prog. Ser.* **346**, 285–297 (2007).
96. Simon, M., Johnson, M., Tyack, P. & Madsen, P. T. Behaviour and kinematics of continuous ram filtration in bowhead whales (*Balaena mysticetus*). *Proc. R. Soc. B Biol. Sci.* **276**, 3819–3828 (2009).
97. Baumgartner, M. F. & Mate, B. R. Summertime foraging ecology of North Atlantic right whales. *Mar. Ecol. Prog. Ser.* **264**, 123–135 (2003).
98. van der Hoop, J. M. et al. Foraging rates of ram-filtering North Atlantic right whales. *Funct. Ecol.* **33**, 1290–1306 (2019).
99. Burnett, J. D. et al. Estimating morphometric attributes of baleen whales with photogrammetry from small UASs: a case study with blue and gray whales. *Mar. Mammal Sci.* **35**, 108–139 (2019).
100. Torres, W. I. & Bierlich, K. C. MorphoMetriX: a photogrammetric measurement GUI for morphometric analysis of megafauna. *J. Open Source Softw.* **5**, 1825 (2020).
101. Johnston, D. W. Unoccupied aircraft systems in marine science and conservation. *Ann. Rev. Mar. Sci.* **11**, 439–463 (2019).
102. Durban, J. W. et al. Photogrammetry of blue whales with an unmanned hexacopter. *Mar. Mammal Sci.* **32**, 1510–1515 (2016).
103. Kelley, D. & Richards, C. *oce: Analysis of Oceanographic Data* R Package v. 1.1 (2019).
104. Dubreuil, J. & Petitgas, P. Energy density of anchovy Engraulis encrasicolus in the Bay of Biscay. *J. Fish Biol.* **74**, 521–534 (2009).
105. Chenowith, E. M. *Bioenergetic and Economic Impacts of Humpback Whale Depredation at Salmon Hatchery Release Sites*. PhD thesis, Univ. Alaska (2018).
106. Werth, A. J. Models of hydrodynamic flow in the bowhead whale filter feeding apparatus. *J. Exp. Biol.* **207**, 3569–3580 (2004).
107. Werth, A. in *Feeding: Form, Function, and Evolution in Tetrapod Vertebrates* (ed. Schwenk, K.) 487–526 (Academic, 2000).
108. Mckinstry, C. A. E., Westgate, A. J. & Koopman, H. N. Annual variation in the nutritional value of stage V Calanus finmarchicus: implications for right whales and other copepod predators. *Endang. Species Res.* **20**, 195–204 (2013).
109. Folkow, L. P., Haug, T., Nilssen, K. T. & Nordy, E. S. Estimated food consumption of minke whales Balaenoptera acutorostrata in Northeast Atlantic waters in 1992-1995. *NAMMCO Sci. Publ.* **2**, 65–80 (2000).
110. Brodie, P. F. Cetacean energetics, an overview of intraspecific size variation. *Ecology* **56**, 152–161 (1975).
111. Hill, S. L. et al. Is current management of the antarctic krill fishery in the atlantic sector of the southern ocean precautionary? *CCAMLR Sci.* **23**, 31–51 (2016).
112. Atkinson, A. et al. Oceanic circumpolar habitats of Antarctic krill. *Mar. Ecol. Prog. Ser.* **362**, 1–23 (2008).
113. Ratnarajah, L., Bowie, A. R., Lannuzel, D., Meiners, K. M. & Nicol, S. The biogeochemical role of baleen whales and krill in Southern Ocean nutrient cycling. *PLoS ONE* **9**, e114067 (2014).
114. Rose, C., Parker, A., Jefferson, B. & Cartmell, E. The characterization of feces and urine: a review of the literature to inform advanced treatment technology. *Crit. Rev. Environ. Sci. Technol.* **45**, 1827–1879 (2015).
115. Candela, E., Camacho, M. V. & Perdomo, J. Iron absorption by humans and swine from Fe (III)-EDTA. Further studies. *J. Nutr.* **114**, 2204–2211 (1984).
116. Ratnarajah, L. et al. A preliminary model of iron fertilisation by baleen whales and Antarctic krill in the Southern Ocean: sensitivity of primary productivity estimates to parameter uncertainty. *Ecol. Modell.* **320**, 203–212 (2016).
117. Twining, B. S., Baines, S. B. & Fisher, N. S. Element stoichiometries of individual plankton cells collected during the Southern Ocean Iron Experiment (SOFeX). *Limnol. Oceanogr.* **49**, 2115–2128 (2004).
118. Strzepek, R. F., Maldonado, M. T., Hunter, K. A., Frew, R. D. & Boyd, P. W. Adaptive strategies by Southern Ocean phytoplankton to lessen iron limitation: uptake of organically complexed iron and reduced cellular iron requirements. *Limnol. Oceanogr.* **56**, 1983–2002 (2011).
119. Quigg, A. et al. The evolutionary inheritance of elemental stoichiometry in marine phytoplankton. *Nature* **425**, 291–294 (2003).
120. Wickham, H. *ggplot2: Elegant Graphics for Data Analysis* 2nd edn (Springer, 2016).
121. Lockyer, C. Body weights of some species of large whales. *ICES J. Mar. Sci.* **36**, 259–273 (1976).
122. Blix, A. S. & Folkow, L. P. Daily energy expenditure in free living minke whales (*Balaenoptera acutorostrata*). *Acta Physiol. Scand.* **153**, 61–66 (1995).
123. Nordoy, E. S., Folkow, L. P., Martensson, P. & Blix, A. S. Food requirements of Northeast Atlantic minke whales. *Dev. Mar. Biol.* **4**, 307–317 (1995).
124. Murase, H., Tamura, T., Matsuoka, K. & Hakamada, T. First attempt of estimation of feeding impact on krill standing stock by three baleen whale species (Antarctic minke, humpback and fin whales) in Areas IV and V using JARPA dat. *Inst. Cetacean Res. Rep.* SC/D06/J22 (2006).
125. Southall, B. L. et al. Behavioral responses of individual blue whales (*Balaenoptera musculus*) to mid-frequency military sonar. *J. Exp. Biol.* **222**, jeb190637 (2019).
126. Goldbogen, J. A. et al. Blue whales respond to simulated mid-frequency military sonar. *Proc. R. Soc. B* **280**, 20130657 (2013).
127. Stimpert, A. K. et al. Sound production and associated behavior of tagged fin whales (*Balaenoptera physalus*) in the Southern California Bight. *Anim. Biotelemetry* **3**, 1–12 (2015).
128. Goldbogen, J. A. et al. Foraging behavior of humpback whales: kinematic and respiratory patterns suggest a high cost for a lunge. *J. Exp. Biol.* **211**, 3712–3719 (2008).
129. Wiley, D. et al. Underwater components of humpback whale bubble-net feeding behaviour. *Behaviour* **148**, 575–602 (2011).
130. Friedlaender, A. S., Tyson, R. B., Stimpert, A. K., Read, A. J. & Nowacek, D. P. Extreme diel variation in the feeding behavior of humpback whales along the western Antarctic Peninsula during autumn. *Mar. Ecol. Prog. Ser.* **494**, 281–289 (2013).
131. Kahane-Rapport, S. R. et al. Lunge filter feeding biomechanics constrain rorqual foraging ecology across scale. *J. Exp. Biol.* **223**, jeb224196 (2020).
132. Friedlaender, A. S. et al. Feeding rates and under-ice foraging strategies of the smallest lunge filter feeder, the Antarctic minke whale (*Balaenoptera bonaerensis*). *J. Exp. Biol.* **217**, 2851–2854 (2014).
133. Domenici, P., Batty, R. S. & Similä, T. Spacing of wild schooling herring while encircled by killer whales. *J. Fish Biol.* **57**, 831–836 (2000).
134. Tamura, T. *et al. Some examinations of uncertainties in the prey consumption estimates of common minke, sei and Bryde's whales in the western North Pacific*. (2009).
135. Innes, S., Lavigne, D. M., Earle, W. M. & Kovacs, K. M. Estimating feeding rates of marine mammals from heart mass to body mass ratios. *Mar. Mammal Sci.* **2**, 227–229 (1986).
136. Armstrong, A. J. & Siegfried, W. R. Consumption of Antarctic krill by minke whales (*Balaenoptera acutorostrata*). *Antarct. Sci. 3(1)13-18. 1991.* **3**, 13–18 (1991).
137. Reilly, S. et al. Biomass and energy transfer to baleen whales in the South Atlantic sector of the Southern Ocean. *Deep. Res. Part II Top. Stud. Oceanogr.* **51**, 1397–1409 (2004).
138. Read, A. J. & Brownstein, C. R. Considering other consumers: Fisheries, predators, and Atlantic herring in the Gulf of Maine. *Conserv. Ecol.* **7** (2003).
139. Nagy, K. Food requirements of wild animals: predictive equations for free-living mammals, reptiles, and birds. *Nutr. Abstr. Rev. Ser. B* **71**, 21R–31R (2001).
140. Stevick, P. T. et al. Trophic relationships and oceanography on and around a small offshore bank. *Mar. Ecol. Prog. Ser.* **363**, 15–28 (2008).

Acknowledgements We would like to thank J. Barlow at NOAA's Southwest Fisheries Science Center for an internal review of our manuscript, and R. Anderson for editorial assistance. D. Cade was integral in the fieldwork and on advising with the methods used in the manuscript. A. Atkinson and O. Schofield advised on the methods relating to Southern Ocean productivity. Illustrations in Fig. 3 were provided by K. Duthie, all other illustrations were provided by A. Boersma. Funding for this work was provided by the National Science Foundation (IOS 1656691, OPP 1644209, 1643877, 1250208, 1440435, PRFB 1906332), the Office of Naval Research Young Investigator Program (N000141612477), the Defense University Research Instrumentation Program (N00014-16-1-2546), the National Geographic Society (EC-53352R-18), the Percy Sladen Memorial Trust, the PADI Foundation, the Society for Marine Mammalogy, Torben og Alice Frimodts Fond, the Volgenau Foundation, the International Fund for Animal Welfare, and MAC3 Impact Philanthropies. Data collection was also supported by NSF Palmer LTER, WWF, OneOcean Expeditions, the Hogwarts Running Club, Cheeseman's Ecology Safaris, and the American Cetacean Society.

Author contributions M.S.S. and J.A.G. conceived and led the project. Data collection and initial processing by S.R.K-R., W.T.G., J.A.F., K.C.B., P.S.S., J.D., G.S.P., D.N.W., J.C., D.W.J., A.S.F., E.L.H. and J.A.G. Data analysed and visualized by M.F.C. and M.S.S. Manuscript drafted by M.S.S. with substantial contributions from M.F.C., E.L.H., N.D.P. and J.A.G. All authors edited and proofread the paper.

Competing interests The authors declare no competing interests.

Additional information

Supplementary information The online version contains supplementary material available at https://doi.org/10.1038/s41586-021-03991-5.

Correspondence and requests for materials should be addressed to Matthew S. Savoca.

Peer review information *Nature* thanks Peter Corkeron, Kimberly Davies, Victor Smetacek and the other, anonymous, reviewer(s) for their contribution to the peer review of this work. Peer reviewer reports are available.

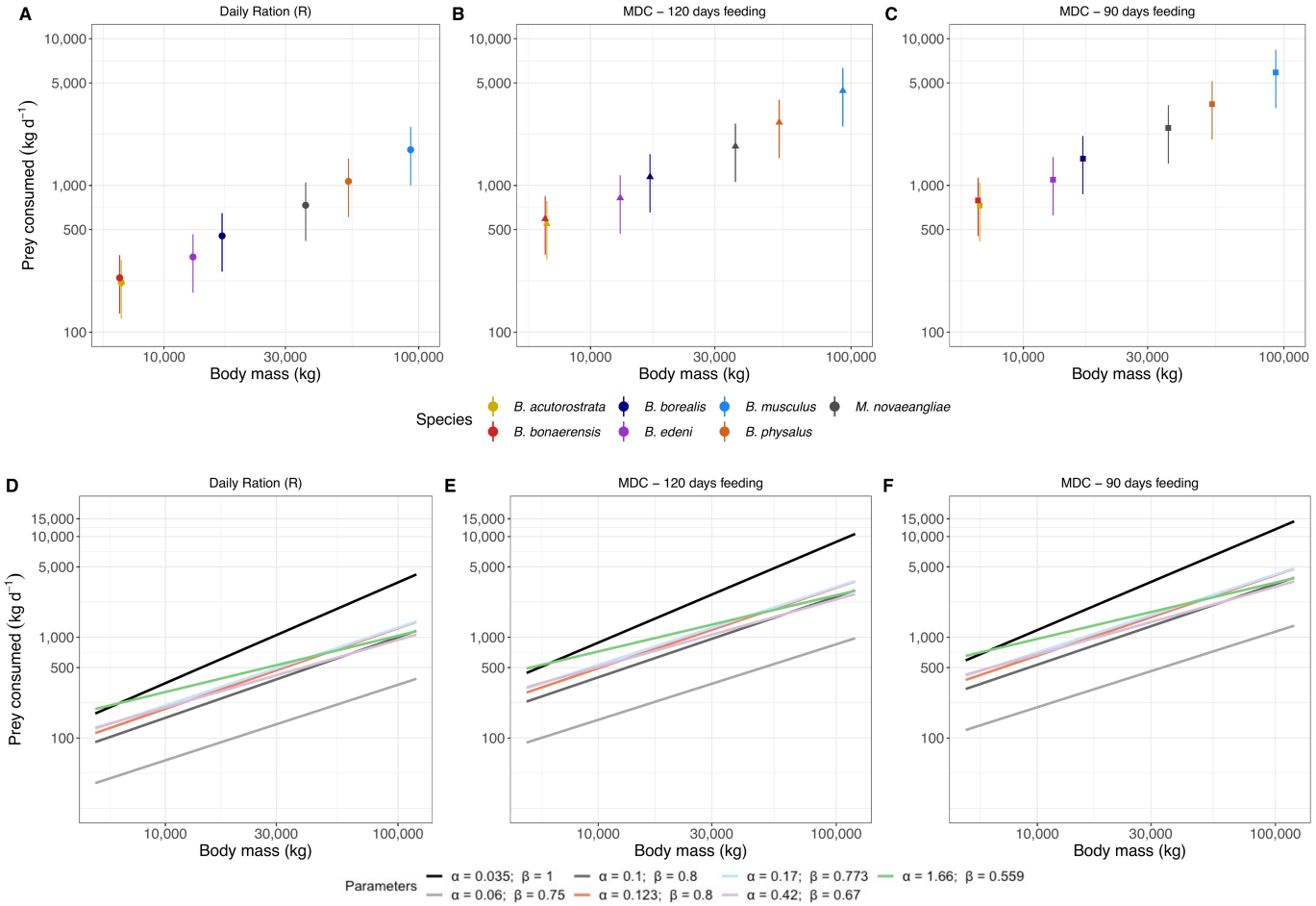

Extended Data Fig. 1 | Prior estimates of daily prey consumption. See Extended Data Table 3 for studies that use specific parameter values plotted in panels **d**, **e** and **f**. **a**, Daily ration (*R*) estimate using equation (1). Note that here *B. edeni* is representative of the Bryde's whale complex that includes *B. brydei*. **b**, Mean daily consumption (MDC) estimate using equation (1) if 120 days spent feeding. **c**, Mean daily consumption (MDC) estimate using equation (1) if 90 days spent feeding. **d**, Daily ration (*R*) estimate using equation (2). **e**, Mean daily consumption (MDC) estimate using equation (2) if 120 days spent feeding. **f**, Mean daily consumption (MDC) estimate using equation (2) if 90 days spent feeding.

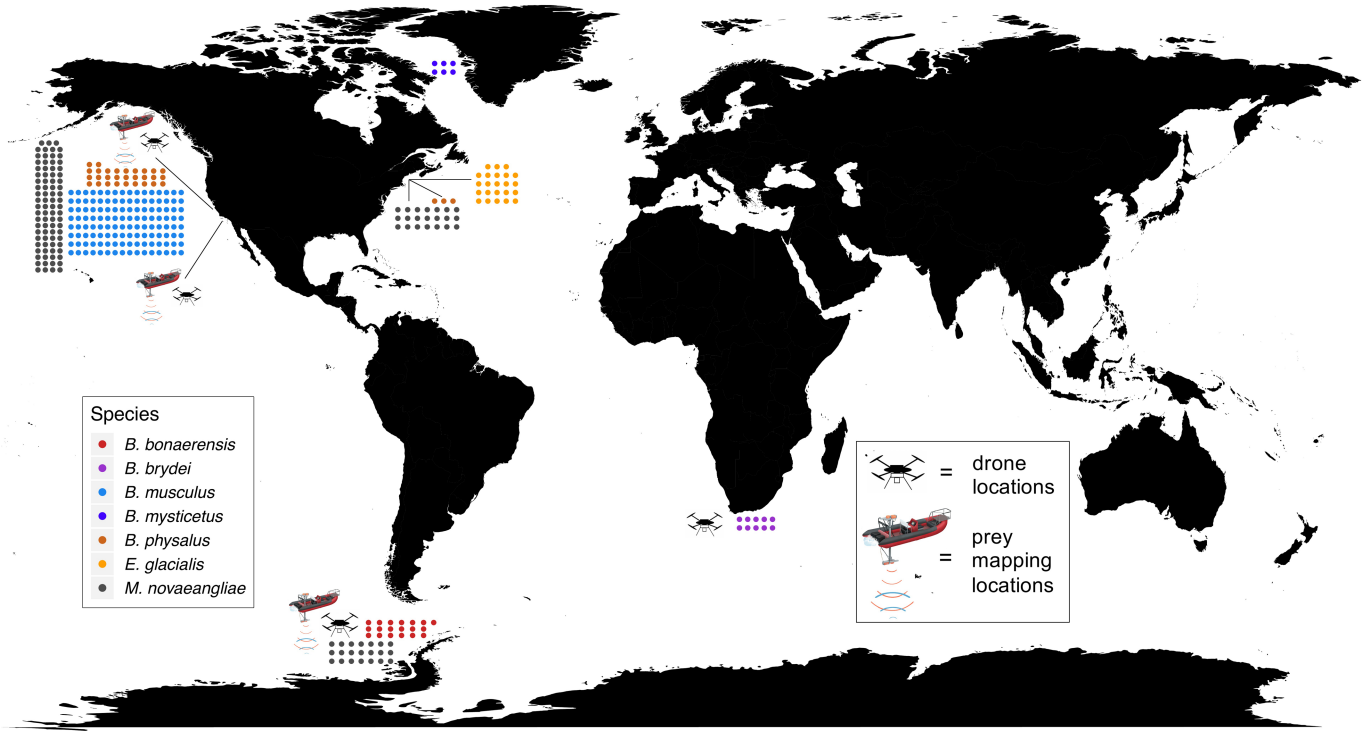

Extended Data Fig. 2 | Map of field data. Each point represents a tag deployment, coloured by species. The world map was generated from ref. [120]. The icons of the RHIB with the echosounder represent regions where we have prey mapping data and were illustrated by Alex Boersma; drone icons indicate where we conducted drone measurements.

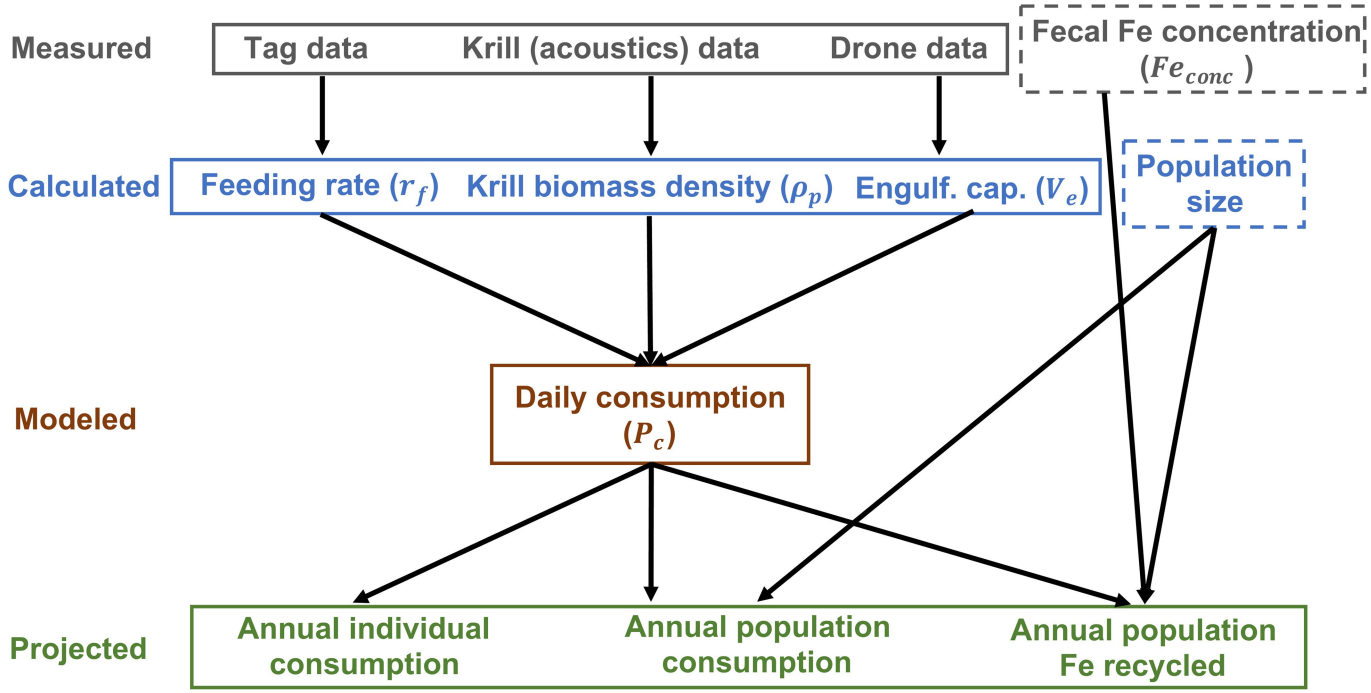

Extended Data Fig. 3 | Analysis flowchart. The outline of the analytical steps from field measurements to modelled daily krill consumption, and finally to projected annual consumption, and nutrients (for example, iron) recycled. Boxes with solid lines are data we collected, modelled and projected; dashed boxes are data we retrieved from other sources. The majority of our data, analyses, results, and inferences focused on krill-feeding rorqual whales (207 of 321 tag deployments), and this flow chart highlights those methods in particular. For details on the measured data, see: Methods sections 'Tagging data' and 'Lunge detection methods' for tag data; Methods section 'Prey methods' for prey data; Methods section 'Drone/engulfment capacity methods' for drone data; Methods section 'Iron recycling and primary production' for fecal iron concentrations. For details on the calculated information from the field data, see: Methods sections 'Rorqual feeding rate methods' and 'Feeding rate validation' for feeding rate (lunges h^{-1}) calculations; Methods section 'Prey methods' for prey biomass calculations; Methods section 'Drone/engulfment capacity methods' for engulfment capacity calculations; Methods section 'Annual and population-level projections' for population size information. For details on the modelled outputs of daily prey ingestion and water filtration, see: Methods section 'Daily prey consumption methods for rorquals' for rorquals; Methods section 'Balaenid water filtration and prey estimation methods' for balaenids. For details on annual projected prey ingested, water filtered and iron recycled see: Methods section 'Annual and population-level projections' for prey ingested; Methods section 'Iron recycling and primary production' for iron recycled. For specific methods on fish-feeding rorquals see the 'Fish' subsection of the 'Prey methods' section, and for specific details on methods regarding balaenids, see the 'Copepod' portion of the 'Prey methods' section as well as section 'Balaenid water filtration and prey estimation methods'.

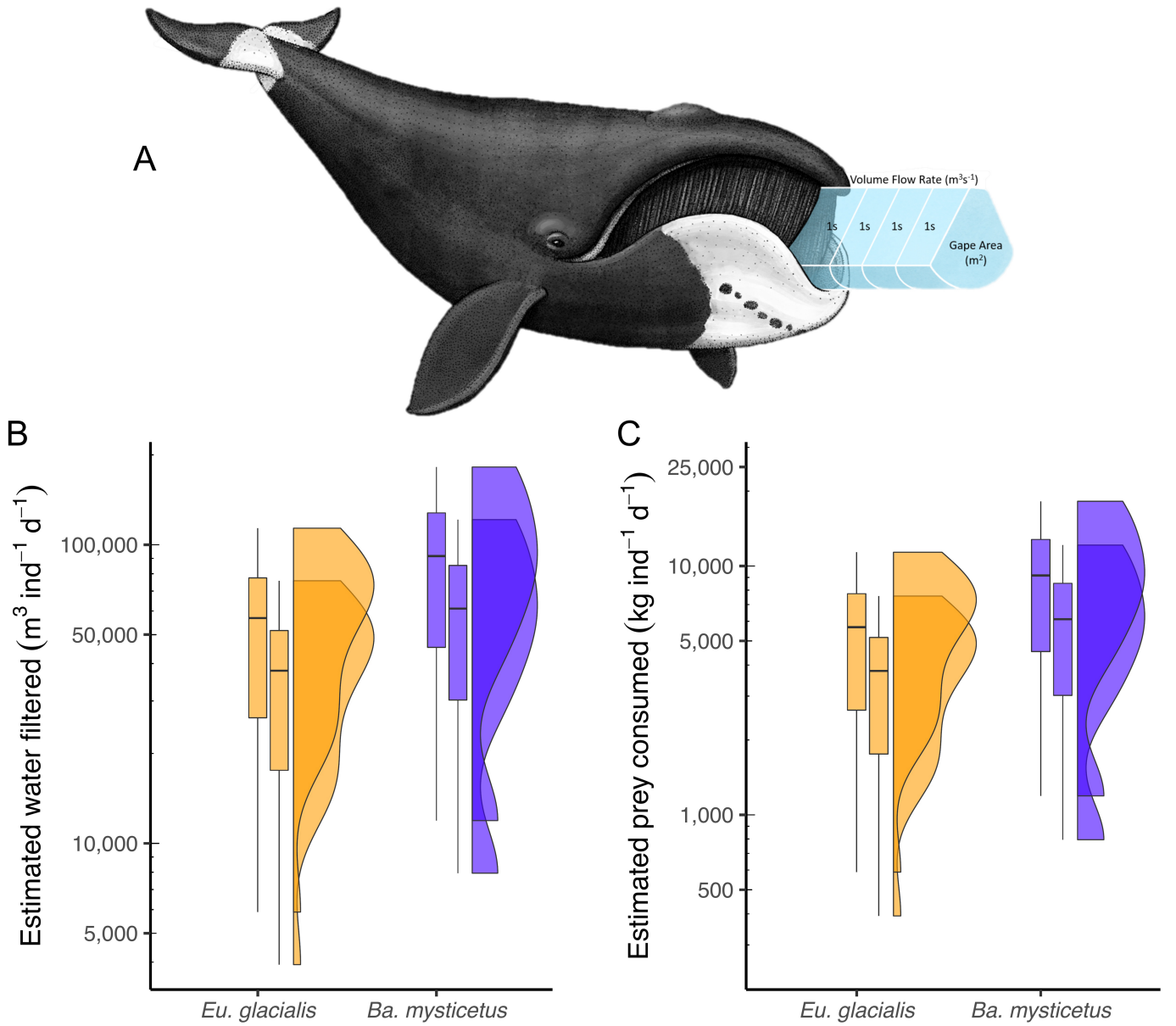

Extended Data Fig. 4 | Balaenid daily water filtration and prey consumption. **a**, Visualization of an example bowhead whale (*Ba. mysticetus*) showing how water filtration was calculated. **b**, Water filtered per day for an individual bowhead (*Ba. mysticetus*) and North Atlantic right whale (*Eu. glacialis*). Density plots illustrate the full scope of all daily simulations with the height representing the relative probability of each output; the boxplots show the quartiles of these outputs with the thick line representing the median and the shaded region representing the Q1–Q3 range (25th–75th percentiles) of all modelled daily rates. For each species, the lower distribution represents a low effort foraging day (10 h feeding) and the higher distribution represents a high effort foraging day (15 h feeding). **c**, Prey consumed per day for an individual bowhead and North Atlantic right whale. Density plots illustrate the full scope of all daily simulations with the height representing the relative probability of each output; the boxplots show the quartiles of these outputs with the thick line representing the median and the shaded region representing the Q1–Q3 range (25th–75th percentiles) of all modelled daily rates. For each species, the lower distribution represents a low effort foraging day (10 h feeding) and the higher distribution represents a high effort foraging day (15 h feeding).

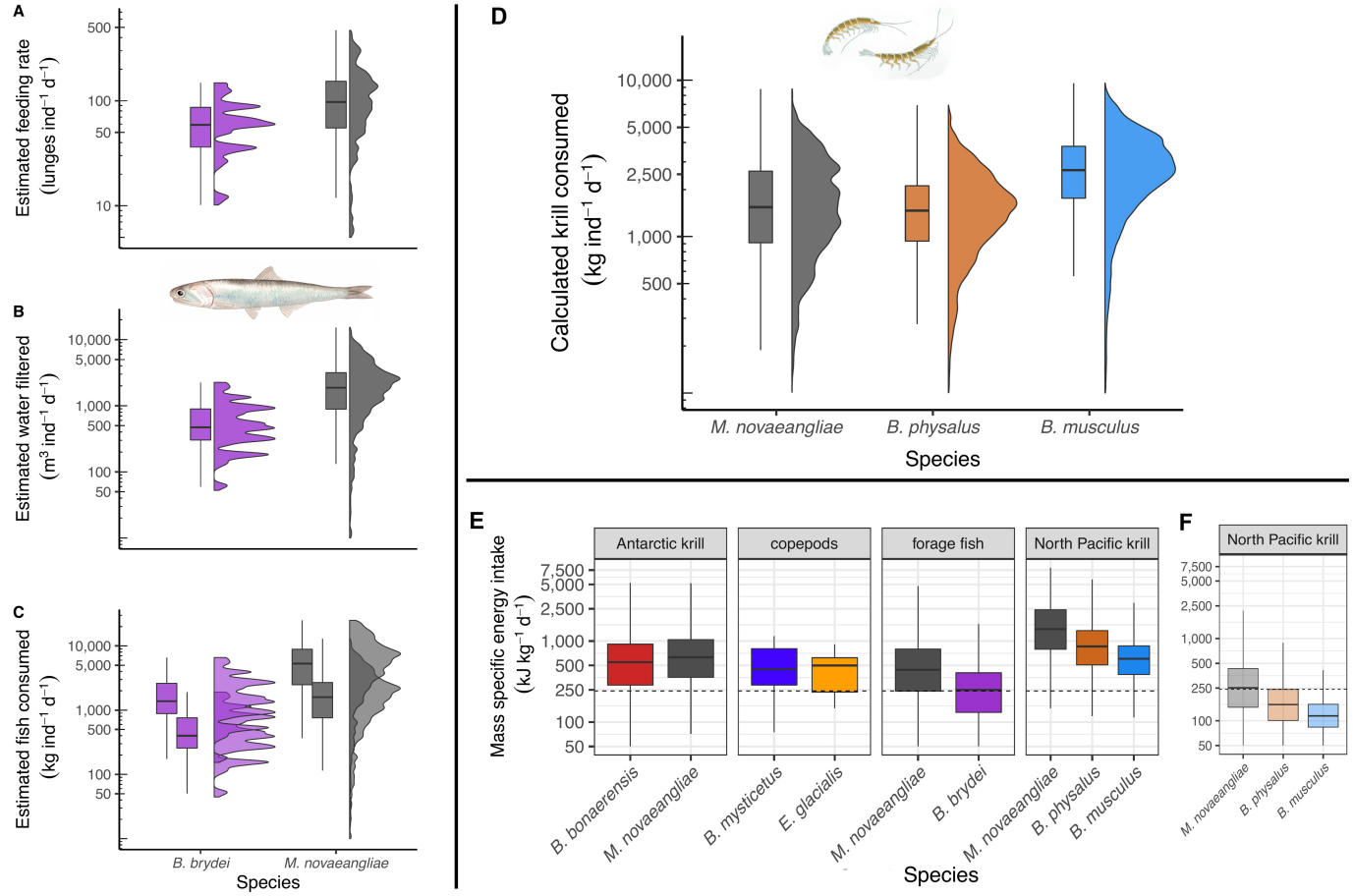

Extended Data Fig. 5 | Additional daily prey consumption results. **a**–**c**, Estimated individual daily feeding rates, filtration volumes and prey consumption for fish-feeding humpback whales (*M. novaeangliae*) from the California Current and North Atlantic Ocean (Stellwagen Bank, Gulf of Maine), as well as for Bryde's whales (*Balaenoptera brydei*) tagged off South Africa. The smaller distributions assume smaller fish schools that are 29% of the size of the engulfment volume (see Methods). Density plots illustrate the full scope of all daily simulations with the height representing the relative probability of each output; the boxplots show the quartiles of these outputs with the thick line representing the median and the shaded region representing the 25th–75th percentiles of all modelled daily rates. **d**, Non-Antarctic humpback, fin (*B. physalus*), and blue whales (*B. musculus*) prey consumption estimates. Density plots illustrate the full scope of all daily simulations with the height representing the relative probability of each output; the boxplots show the quartiles of these outputs with the thick line representing the median and the shaded region representing the 25th–75th percentiles of all modelled daily rates. **e**, Mass-specific daily energy intake. Species-specific average whale mass was calculated using our drone-length measurements (Extended Data Table 1), converting to body weight according to ref. [121]. Average prey energy density for Antarctic krill, eastern North Pacific krill (2 spp.), forage fish, and copepods described in sections 'Daily prey consumption methods for rorquals' and 'Balaenid water filtration and prey estimation methods'. Dashed horizontal line represents 80 kJ kg^{-1} d^{-1} (converted to 242.36 kJ kg^{-1} d^{-1} via MDC methodology), which previous studies have used to estimate mysticete prey consumption[122–124]. Boxplots show the quartiles of all modelled daily outputs with the thick line representing the median and the shaded region representing the 25th–75th percentiles of all modelled daily rates. **f**, Mass-specific daily energy intake using Antarctic krill TS–L equations for North Pacific krill, as has been used in previous studies[74,83,86]. Boxplots show the quartiles of all modelled daily outputs with the thick line representing the median and the shaded region representing the 25th–75th percentiles of all modelled daily rates. Dashed horizontal line represents 80 kJ kg^{-1} d^{-1} (converted to 242.36 kJ kg^{-1} d^{-1} via MDC methodology), which previous studies have used to estimate mysticete prey consumption[122–124]. Falling largely below the horizontal dashed line, this level of prey consumption would probably not be possible for these rorqual species to meet their energetic demands.

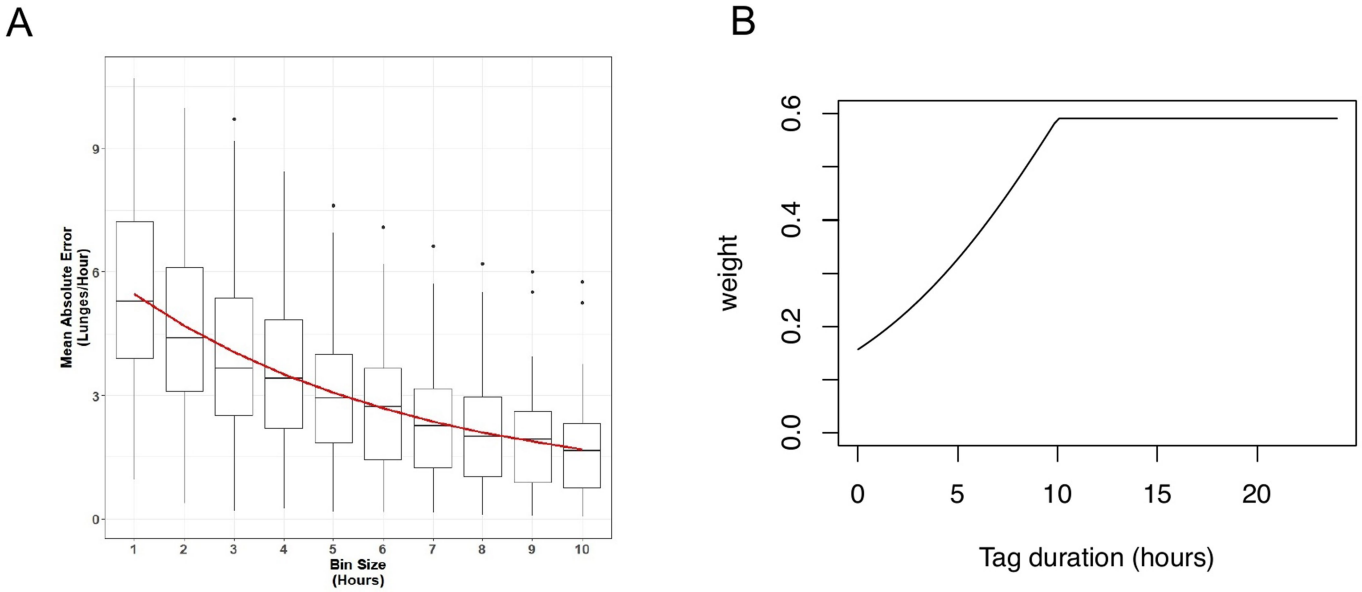

Extended Data Fig. 6 | Feeding rate validation measurements and weighting curve. a, Using medium term tags attached to ENP blue whales (*B. musculus*), we calculated the mean absolute error in daily lunge rate estimation when randomly subsampling and quantifying hourly lunge rates from different duration blocks of multi-day tag deployments. This analysis showed that the longer a sub-daily deployment is, the more accurate and precise it becomes in estimating the daily lunge rate. **b**, Using data from panel **a**, we generated a custom weighting function which we applied to all deployments in our dataset, accounting for our increased confidence in the lunge rates of longer deployments. Deployments ≥10 h were weighted equally.

Extended Data Table 1 | Summary of baleen whale data measured, calculated, and modelled

Species	Study area(s) Extended Data Fig. 2	Num. tagged Extended Data Fig. 2	Num. sized	Total length in m	Engulfment capacity in m^3 (V_e)	Prey biomass density* in kg m^{-3} (ρ_p)	Daily feeding rate in lunges d^{-1} (n_f daily) Fig. 2	Daily prey consumption in kg d^{-1} (P_C) Fig. 2
Balaenoptera musculus	Northern California[25,75,84] Southern California[125,126]	125	42	22.52 (21.67-23.07)	86.19 (74.88-94.20)	μ: 0.63 σ: 2.46	204 (138-270)	15904 (10452-21952)
Balaenoptera physalus	Northern California[25] Southern California[74,127] Gulf of Maine	32	9	18.15 (16.67-19.33)	41.03 (30.37-51.30)	krill μ: 0.62 σ: 2.50	222 (159-302)	8192 (5079-12162)
Megaptera novaeangliae	Northern California[1,25,87,128] Southern California[25,87,128] Gulf of Maine[129] West Antarctic Peninsula[130,131]	108	90	11.76 (10.56-12.71)	21.04 (14.85-27.08)	ENP krill μ: 0.61 σ: 2.51 ENP fish 7.8 WAP μ: 0.19 σ: 2.17	ENP krill 546 (296-812) ENP fish 92 (49-148) WAP 622 (402-914)	ENP krill 9039 (5417-15103) ENP fish low: 1554 (707-2653) high: 5353 (2436-9141) WAP 3151 (1813-4926)
Balaenoptera bonaerensis	West Antarctic Peninsula[25,131,132]	17	40	8.06 (7.03-8.65)	3.21 (2.10-4.01)	krill μ: 0.15 σ: 2.05	1207 (849-1615)	685 (362-1085)
Balaenoptera brydei	Southern South Africa	10	2	12.04 (11.00-13.08)	10.19 (7.67-12.70)	fish 7.8	59 (36-87)	low: 400 (256-760) high: 1378 (884-2617)
Balaena mysticetus	West Greenland[80]	6	NA	NA	NA	copepods[95] 0.006	NA	low: 4748 (3021-8522) high: 7122 (4532-12783)
Eubalaena glacialis	Gulf of Maine[78,79]	23	NA	NA	NA	copepods[97,98] 0.17	NA	low: 3786 (1756-5160) high: 5679 (2634-7741)

Values presented are the median, with the Q1–Q3 range in parentheses (25th–75th percentile), unless otherwise specified. ENP, eastern North Pacific; WAP, West Antarctic Peninsula. Original sources for previously processed data is provided in the Study Areas column[25,74,76,78,79,84,87,96,125–132].

*For *B. musculus*, *B. physalus*, *M. novaeangliae*, and *B. bonaerensis*, μ represents the geometric mean and σ represents the geometric standard deviation of the lognormally distributed krill biomass densities measured in patches near foraging whales (scaling). For *B. brydei* and the subset of *M. novaeangliae* that fed on fish, we used a previously published biomass density of forage fish schools[87,94,133]. For balaenids (*Ba. mysticetus* and *Eu. glacialis*) we used estimates of copepod densities from previously published studies[95–98]. See prey data methods (section 'Prey methods') for more details.

Extended Data Table 2 | Calculations to estimate primary production stimulated by whale recycled iron in the Southern Ocean

Parameter	Value or calculation	Result	Uncertainty (range)	Reference
Annual whale-recycled iron	12,000 tonnes Fe yr^{-1}		7,000-15,000 tonnes Fe yr^{-1}	Present study
Whale-recycled iron incorporated by Southern Ocean phytoplankton	(12,000 tonnes Fe yr^{-1}) × 0.25	3,000 tonnes = 3 × 10^9 g Fe yr^{-1}	750-6,750 tonnes Fe yr^{-1}	[40]
Fe : C ratio in Southern Ocean phytoplankton	3 µmol Fe : mol C		1-6 µmol Fe : mol C	[117–119]
Converting whale-recycled iron from tonnes to µmol	(3 × 10^9 g Fe) × (0.018 mol Fe : g Fe) × (1 × 10^6 µmol mol^{-1})	5.37 × 10^{13} µmol Fe recycled annually by whales	1.35-12.15 × 10^{13} µmol Fe†	Present study
Whale-recycled iron to NPP (carbon incorporated by phytoplankton)	(5.37 × 10^{13} µmol Fe) × (mol C : 3 µmol Fe) × (12.01 g C : mol C)	2.15 × 10^{14} g C yr^{-1} = 215 Tg C yr^{-1} incorporated by phytoplankton	27-1,459 Tg C yr^{-1} ‡	Present study
Enhancement of Southern Ocean NPP from whale-recycled iron	215 Tg C yr^{-1} ÷ 1949 Tg C yr^{-1} #	11% annual enhancement of Southern Ocean NPP by whale-recycled iron	1.4-74.9%	Present study

†Range from the uncertainty of iron recycled by whales that is incorporated by phytoplankton (750–6,750 tonnes yr^{-1}) from line 1.
‡Range from the uncertainty of iron recycled by whales and uncertainty in Fe:C ratio in Southern Ocean diatoms from line 3.
#1,949 Tg C yr^{-1} is the mean annual Southern NPP from 1997–2006 from ref. [44]. Data from refs. [40,117–119].

Extended Data Table 3 | Parameters used to estimate mysticete prey consumption

α	β	Reference(s)
0.1	0.8	6,134
0.42	0.67	27,52,55,134–136
0.035	1	52,54
1.66	0.559	53,137
0.123	0.8	58,138
0.17	0.773	27,139
0.06	0.75	19,51,140

Studies that have used equation (2) to estimate mysticete prey consumption and the parameters used to populate their models. Data from refs. [6,8,20,51,63–65,68–70,134–140].

Extended Data Table 4 | Summary of tag deployments

Species	Tag type	Num. deployments	Tag time (hours)	Num. with prey mapping	Num. with video
Balaenoptera bonaerensis	CATS	17	12.94 (7.36-27.80)	16	16
Balaenoptera brydei	CATS	10	4.72 (2.73-10.76)	NA	5
Balaenoptera physalus	CATS	7	0.74 (0.17-3.88)	3	2
Balaenoptera physalus	DTAG	19	4.62 (3.72-5.83)	9	NA
Balaenoptera physalus	Medium duration	6	76.57 (62.63-96.32)	NA	NA
Balaenoptera musculus	CATS	50	7.78 (2.63-20.21)	13	19
Balaenoptera musculus	DTAG	59	4.61 (2.56-5.55)	27	NA
Balaenoptera musculus	Medium duration	16	109.46 (98.97-234.83)	NA	NA
Megaptera novaeangliae	CATS	108	5.87 (3.05-11.72)	54	57
Balaena mysticetus	DTAG	6	0.57 (0.37-0.95)	NA	NA
Eubalaena glacialis	DTAG	23	1.34 (0.88-3.18)	NA	NA

Values presented for the tag duration for all tag deployments used in this study are the median, with the Q1–Q3 range in parentheses (25th–75th percentile). Number of tag deployments with concurrent prey mapping (krill-feeding whales only) measurements and video of feeding events are also listed. A subset of these tag deployments have been previously published, see Extended Data Table 1 for references.

nature research

Corresponding author(s): Matthew Savoca

Last updated by author(s): Jul 5, 2020

Reporting Summary

Nature Research wishes to improve the reproducibility of the work that we publish. This form provides structure for consistency and transparency in reporting. For further information on Nature Research policies, see our Editorial Policies and the Editorial Policy Checklist.

Statistics

For all statistical analyses, confirm that the following items are present in the figure legend, table legend, main text, or Methods section.

n/a	Confirmed	
☐	☒	The exact sample size (*n*) for each experimental group/condition, given as a discrete number and unit of measurement
☐	☒	A statement on whether measurements were taken from distinct samples or whether the same sample was measured repeatedly
☒	☐	The statistical test(s) used AND whether they are one- or two-sided *Only common tests should be described solely by name; describe more complex techniques in the Methods section.*
☒	☐	A description of all covariates tested
☐	☒	A description of any assumptions or corrections, such as tests of normality and adjustment for multiple comparisons
☐	☒	A full description of the statistical parameters including central tendency (e.g. means) or other basic estimates (e.g. regression coefficient) AND variation (e.g. standard deviation) or associated estimates of uncertainty (e.g. confidence intervals)
☒	☐	For null hypothesis testing, the test statistic (e.g. *F*, *t*, *r*) with confidence intervals, effect sizes, degrees of freedom and *P* value noted *Give P values as exact values whenever suitable.*
☒	☐	For Bayesian analysis, information on the choice of priors and Markov chain Monte Carlo settings
☒	☐	For hierarchical and complex designs, identification of the appropriate level for tests and full reporting of outcomes
☒	☐	Estimates of effect sizes (e.g. Cohen's *d*, Pearson's *r*), indicating how they were calculated

Our web collection on statistics for biologists contains articles on many of the points above.

Software and code

Policy information about availability of computer code

Data collection	Field data from our instruments were downloaded and stored in Microsoft Excel 2016, and later analyzed in Echoview (for acoustic data), Matlab 2014, and R v. 3.6
Data analysis	The code for this paper's results, figures can be found at our GitHub repository: https://github.com/mssavoca/prey_consumption_paper;

For manuscripts utilizing custom algorithms or software that are central to the research but not yet described in published literature, software must be made available to editors and reviewers. We strongly encourage code deposition in a community repository (e.g. GitHub). See the Nature Research guidelines for submitting code & software for further information.

Data

Policy information about availability of data

All manuscripts must include a data availability statement. This statement should provide the following information, where applicable:

- Accession codes, unique identifiers, or web links for publicly available datasets
- A list of figures that have associated raw data
- A description of any restrictions on data availability

Code to reproduce the figures and analyses in this paper are available at: https://github.com/mssavoca/prey_consumption_paper; all data and code are available on Github.

Field-specific reporting

Please select the one below that is the best fit for your research. If you are not sure, read the appropriate sections before making your selection.

☐ Life sciences ☐ Behavioural & social sciences ☒ Ecological, evolutionary & environmental sciences

For a reference copy of the document with all sections, see nature.com/documents/nr-reporting-summary-flat.pdf

Ecological, evolutionary & environmental sciences study design

All studies must disclose on these points even when the disclosure is negative.

Study description	Study included
Research sample	Fieldwork consisted of attaching tags (n = 321) to baleen whales in the wild, and also to measure the whales length by aerial drone and the dynamics of the prey patch using active acoustics from a small vessel.
Sampling strategy	Fieldwork consisted of attaching tags (n = 321) to baleen whales in the wild, and also to measure the whales length by aerial drone and the dynamics of the prey patch using active acoustics from a small vessel. Whales were tagged opportunistically on their foraging grounds.
Data collection	Members of the research team (the paper's authors) collected, processed, and analyzed the field data described above and in detail i, the Methods section.
Timing and spatial scale	Fieldwork and analysis was conducted from 2010-2019. Our field sites for this study included the California Current, coastal South Africa, Stellwagen Bank National Marine Sanctuary, western Greenland, and the western Antarctic Peninsula (see Fig. S3 in paper).
Data exclusions	Tag deployments that did not include any feeding behavior were excluded as we were interested in calculating foraging behavior (feeding lunges, prey consumed) given it was a day that the animal as feeding. More details are provided in the Methods section.
Reproducibility	All of our methods of fieldwork, data processing and analysis, and inference are described in detail in paper. Substantial detail is provided such that our study could be replicated if desired.
Randomization	This study did not consist of a controlled experiment; randomization was not necessary.
Blinding	This study did not consist of a controlled experiment; blinding was not necessary.

Did the study involve field work? ☒ Yes ☐ No

Field work, collection and transport

Field conditions	Fieldwork was conducted on days where weather permitted small boat operations (i.e., minimal to moderate wind and swell). Field seasons are the summer months in each hemisphere.
Location	Our field sites were baleen whale feeding grounds in the California Current, coastal South Africa, Stellwagen Bank National Marine Sanctuary, western Greenland, and the western Antarctic Peninsula (see Fig. S3 in paper).
Access & import/export	All fieldwork was conducted with proper permitting. National Marine Fisheries Service permits 16111, 14809, 19116, 21678, 20430, and National Marine Sanctuary permits MULTI-2017-007 and MULTI-2019-009
Disturbance	Other than tagging the whales, a distance of 50m+ was kept at all times. As we were interested in capturing natural foraging behavior, minimizing disturbance to the animals was paramount for our objectives.

Reporting for specific materials, systems and methods

We require information from authors about some types of materials, experimental systems and methods used in many studies. Here, indicate whether each material, system or method listed is relevant to your study. If you are not sure if a list item applies to your research, read the appropriate section before selecting a response.

Materials & experimental systems

n/a	Involved in the study
☒	☐ Antibodies
☒	☐ Eukaryotic cell lines
☒	☐ Palaeontology and archaeology
☐	☐ Animals and other organisms
☒	☐ Human research participants
☒	☐ Clinical data
☒	☐ Dual use research of concern

Methods

n/a	Involved in the study
☒	☐ ChIP-seq
☒	☐ Flow cytometry
☒	☐ MRI-based neuroimaging

Animals and other organisms

Policy information about studies involving animals; ARRIVE guidelines recommended for reporting animal research

Laboratory animals	No laboratory animals were used in this study.
Wild animals	Fieldwork consisted of attaching tags to baleen whales in the wild, and also to measure the whales length by aerial drone and the dynamics of the prey patch using active acoustics from a small vessel. All fieldwork was conducted with proper permitting. National Marine Fisheries Service permits 16111, 14809, 19116, 21678, 20430, and National Marine Sanctuary permits MULTI-2017-007 and MULTI-2019-009
Field-collected samples	We did not perform analyses on samples collected from the field in this study, only on data collected by drone, echosounder, and the tags themselves.
Ethics oversight	Research was conducted in accordance with Stanford University's IACUC (# 30123)

Note that full information on the approval of the study protocol must also be provided in the manuscript.